buildings

MDPI

Article

Experimental and Computational Assessment of Building Structures Reinforced with Textile Fiber Waste to Improve Thermo-Mechanical Performance

Rabeb Ayed [1,*], Emiliano Borri [2], Safa Skouri [1], Mohamed Lachheb [3], Salwa Bouadila [1], Zohir Younsi [3], Luisa F. Cabeza [2] and Mariem Lazaar [1]

[1] Centre de Recherches et des Technologies de l'Energie, Hamam Lif 2050, Tunisia; skouri_safa@yahoo.fr (S.S.); salwa.bouadila@crten.rnrt.tn (S.B.)
[2] GREiA Research Group, Universitat de Lleida, Pere de Cabrera s/n, 25001 Lleida, Spain; emiliano.borri@udl.cat (E.B.); luisaf.cabeza@udl.cat (L.F.C.)
[3] ICL, Junia, Université Catholique de Lille, LITL, 59000 Lille, France; mohamed.lachheb@junia.com (M.L.); zohir.younsi@junia.com (Z.Y.)
* Correspondence: ayedrabeb09@gmail.com

Abstract: Faced with the growing demand for energy-efficient construction and the need to address environmental challenges, the building sector must innovate to reduce energy consumption and promote sustainability. This study investigates a dual solution to these challenges by enhancing the thermo-mechanical performance of building materials through the integration of textile fiber waste, using a combination of experimental and computational methodologies. This investigation focused on incorporating textile fiber wastes in cementitious composites for construction applications. A series of mechanical and thermal tests were carried out on the cement mortars with different proportions of incorporated textile fibers after 7 and 28 days of water curing. The results showed that the incorporation of fibers can significantly improve the thermal insulation of buildings by reducing the thermal conductivity of cement mortar by up to 52%. To complement experimental findings, computational models were developed using COMSOL Multiphysics 6.2 software to predict the thermal diffusivity and volumetric heat capacity of textile-reinforced mortars. These models revealed that mortars incorporating 40% textile fibers as a sand replacement achieved significant reductions in thermal conductivity, thermal diffusivity, and volumetric heat capacity by approximately 40%, 21%, and 23%, respectively, compared with ordinary cement mortar. Furthermore, this study numerically examined the potential of combining textile-reinforced mortar with phase-change material (PCM) in building applications. The aim of the research was to overcome the challenges of cooling buildings in scorching summer conditions. The optimization of roof and wall composition was based on an assessment of air temperature variation within a space.

Keywords: textile fibers; cement mortar; thermal insulation; experimental study; building applications; phase-change materials

check for updates

Academic Editor: Antonio Caggiano

Received: 2 January 2025
Revised: 25 January 2025
Accepted: 26 January 2025
Published: 29 January 2025

Citation: Ayed, R.; Borri, E.; Skouri, S.; Lachheb, M.; Bouadila, S.; Younsi, Z.; Cabeza, L.F.; Lazaar, M. Experimental and Computational Assessment of Building Structures Reinforced with Textile Fiber Waste to Improve Thermo-Mechanical Performance. *Buildings* **2025**, *15*, 425. https://doi.org/10.3390/buildings15030425

Copyright: © 2025 by the authors. Licensee MDPI, Basel, Switzerland. This article is an open access article distributed under the terms and conditions of the Creative Commons Attribution (CC BY) license (https://creativecommons.org/licenses/by/4.0/).

1. Introduction

In the construction industry, the diverse impacts of petroleum products on climate change, the environment, and human well-being have created a compelling need for innovative solutions and responses [1,2]. This mandate has led the construction sector to embark on a transformative journey towards sustainable practices that not only improve the quality of life but also mitigate the environmental impact of construction in the face of climate

change [3]. To strengthen these efforts, it is essential to provide quantifiable data, such as reductions in carbon emissions (e.g., percentage decrease over a specified period), the amount of recycled materials used, or improvements in energy efficiency achieved through these practices. In addition, the emergence of the concept of "sustainable construction" has led to significant paradigm shifts in various areas, covering the production of building materials, the construction process, building use, demolition, and final disposal [4–6]. The goal of sustainable construction is to minimize a building's ecological footprint throughout its lifecycle, promote a harmonious connection with the environment, and prioritize the well-being of its occupants [7].

Against this backdrop, numerous countries have enacted policies and established government or private entities to regulate, guide, and certify construction practices according to precise and defined standards [8]. The European Union Construction Products Regulation (CPR) sets harmonized standards for building materials to ensure safety, performance, and sustainability [9]. In the United States, the Leadership in Energy and Environmental Design (LEED) certification system promotes sustainable building practices [10], while the International Code Council (ICC) provides building codes that include energy efficiency and environmental guidelines [11]. In addition, countries such as Japan have specific seismic design standards that address the resilience of structures in earthquake-prone areas.

The overall goal of these efforts is to reduce environmental impact and increase the energy efficiency of buildings. This comprehensive approach considers the entire lifecycle of a building, including an assessment of the environmental impact of the inputs and materials used in construction, from their origin and processing to their influence and impact during use and dismantling. In addition, the energy savings achieved in both manufacturing and use are considered, as well as their impact during demolition and the potential for reuse of these inputs and materials [5,6]. The fundamental concept of resource-conscious design in material use is at the heart of "sustainable construction", which ultimately aims to uphold the fundamental principles of transitioning towards a circular economy [12,13].

In this study, a keyword analysis of studies related to the circular economy was employed to yield a reproducible and comprehensible analysis of this research domain [14]. VOSviewer 1.6 software was used to construct the keyword co-occurrence network [15], as depicted in Figure 1. The node size in the network graph corresponds to keyword frequency, while the spatial arrangement of terms on the map indicates their relative associations. This bibliometric map was generated with a minimum threshold of 40 keyword occurrences, resulting in 5903 links (4600 links for the period 2013–2023). The map reveals four distinct clusters: (1) energy conservation and energy; (2) efficiency in buildings, recycling, waste management, and alternative building materials; (3) sustainable development; and (4) green buildings and green supply chain in the construction industry, as well as the circular economy in urban areas.

Group #1, marked in red on Figure 1, is the most significant cluster, comprising 20 keywords. This group primary focus revolves around energy and energy efficiency, along with associated environmental concerns, as indicated by terms such as "energy conservation", "energy", "energy efficiency", "renewable energy", "energy consumption", "energy management", "energy saving", "energy performance", and "embodied energy". Paying close attention to energy usage in buildings is essential, as the residential and industrial building sectors collectively account for over one-third of global energy consumption, as reported by the International Energy Agency (IEA). The building sectors are collectively responsible for more than 30% of global energy consumption and nearly 40% of total direct and indirect carbon dioxide (CO_2) emissions [16]. A significant portion of this energy goes into maintaining thermal comfort in air-conditioned spaces [17–19]. In light of the energy consumption challenges, implementing energy-saving measures, such as enhancing the thermal performance of building elements through thermal insulation, has become a neces-

sity [20–22]. Furthermore, the ongoing increase in energy demand within the construction industry and buildings underscores the urgency of energy efficiency measures. Notably, the COVID-19 pandemic has posed challenges to these endeavors, jeopardizing progress on multiple fronts, including energy consumption policies [23,24]. A high-performance building envelope remains a prerequisite for curbing energy consumption, further underscoring the significance of implementing thermal insulation to mitigate energy losses [20,25].

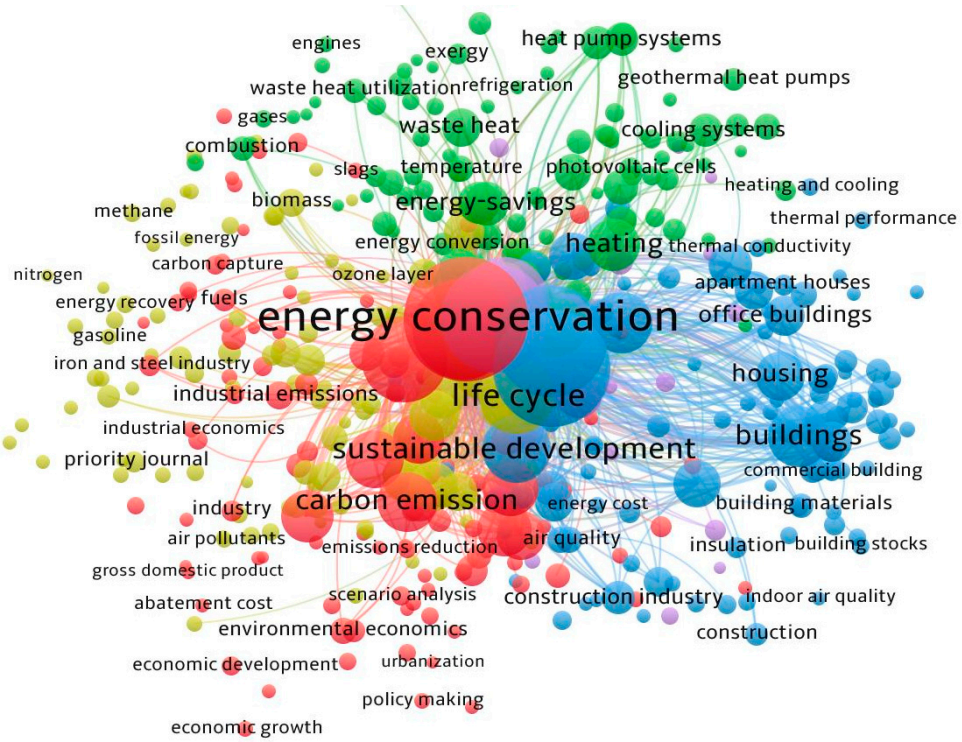


Figure 1. Co-occurrence of research keywords related to circular economy in buildings (2013–2024).

Group #2, depicted in blue on Figure 1, also represents a large cluster consisting of 17 keywords. This group primarily focuses on building efficiency. This focus is represented by terms such as: "building energy", "cement mortar", "concrete", "retrofitting", "refurbishment". "green buildings", "green supply chain", "construction industry", "sustainable design", and "environmental sustainability". This suggests that carrying out energy-efficient renovations of existing buildings, as well as the renovation and rehabilitation of structures, can help address the group's concerns. Improving energy efficiency is probably the most appropriate strategy for extending the lifespan of buildings, resulting in improved living conditions, lower energy costs for occupants [26], and a reduction in the environmental impacts associated with the construction and operation of buildings [27]. This cluster of articles centers on the concept of buildings and a sustainable supply chain within the construction industry, with an emphasis on their ecological principles, resource efficiency, and positive effects on occupant well-being [28]. They typically consume significantly fewer resources than traditional buildings while promoting productivity, comfort, and occupant satisfaction by providing high-quality thermal comfort [29,30].

Group #3, shown in green, includes 13 nodes. This cluster mainly focuses on recycling, waste management, and alternative building materials in the construction industry, indicated by the presence of terms such as: "recycling", "waste management", "recycling materials", "recycling and reuse", "wastes", and "building materials". Numerous studies focusing on recycling and waste reduction argue for significantly reducing the environmental impact associated with waste by producing long-lasting products and encouraging

greater use of reused or recycled materials/systems rather than relying on natural resources during the production phase [31]. These recycledmaterials can serve as substitutes for traditional aggregates in construction materials, such as cement and sand. Notably, cement production accounts for an estimated 5 to 7% of CO_2 emissions generated by human activities. Substituting cement with materials like fly ash or other pozzolanic substances in concrete or mortar production can significantly reduce its carbon footprint [32]. According to Nunez et al. [33], waste management is a pivotal aspect for assessing the circular economy in the construction sector and can be quantified through reduced production of hazardous waste, efficient waste management, and the utilization of a solid waste inventory for the manufacturing process. In the context of mitigating heat loss, the integration of fibers into building materials has demonstrated its effectiveness in reducing thermal conductivity. This approach proves to be a valuable solution for diminishing heat loss [34]. Several studies have been carried out to develop new cementitious composites containing reinforcing materials to improve the overall thermal performance, such as recycled concrete aggregate [35], rubber [36,37], rice mill plant [38], polyethylene [39], lime mud [40], foam [41], vegetable synthetic sponge [42], diatomite [43], glass-ceramic [44] waste bagasse [45], plastic waste [46], silica aerogel [47], cork [48], waste glass [49], and vermiculite [50–52]. Fayed et al. [53,54] have examined the impact of block size on the bearing strength of steel fiber-reinforced recycled aggregate concrete, illustrating how these factors influence the structural integrity of concrete in various applications. Additionally, innovative approaches, like the inclusion of rubber fibers from waste tires in reinforced concrete beams, have demonstrated improved bending and shear performance, providing the dual benefits of enhancing concrete's mechanical properties while contributing to waste tire recycling, as shown by Ecemiş et al. [55]. Similarly, advancements in improving the bond performance between ribbed steel bars and recycled aggregate concrete have revealed that confinement with steel mesh fabrics can significantly enhance the mechanical properties of these materials, according to Zhu et al. [56].

Group #4, highlighted in yellow in Figure 1, includes 15 key terms. The main goal of this cluster is sustainability by offering solutions to reduce environmental impacts. The circular economy model is considered a means of achieving sustainability, as the terms state: "environment", "climate change", "green economy", "low carbon", "circular economy", "material flow analysis", "sustainable cities", and "industrial ecology." Industrial ecology examines industrial systems and aims to identify and implement strategies for reducing their environmental impacts. A sustainable building should adopt a three-fold approach that takes into account the economic, social, and environmental aspects throughout the building lifecycle [57]. Constructing sustainable buildings with high performance and low environmental impact can be achieved at various levels, including sustainable materials, sustainable operations, sustainable services, and sustainable consumption. It is important to highlight the importance of two controversial topics, namely technology and innovation, in achieving sustainability. By linking economic growth with cutting-edge technology, innovation plays a central role, as it can provide solutions to push the boundaries of economic growth while considering the finite availability of resources [58]. The main goal of this cluster is green buildings and a green supply chain applied to the construction industry, as indicated by terms such as "green buildings", "green supply chain", "construction industry", "sustainable design", and "environmental sustainability". Green buildings are designed and constructed based on ecological principles and have minimal impact on the natural environment and human health. They typically consume fewer resources than traditional buildings and enhance the productivity, comfort, and satisfaction of occupants by providing high-quality thermal comfort.

Overall, the key research areas were primarily related to the measures of adopting the circular economy, policies, and frameworks at various levels such as countries, regions, etc.,

as well as the environmental aspects of the circular economy [12,13,33,59]. Subsequently, researchers shifted their focus to the challenges of circular economy-driven design as an early measure to promote circularity, such as using design for disassembly and deconstruction with design tools [36,60–62]. Recently, researchers have primarily focused on material selection, aiming to choose or substitute building materials with circular materials, the development of circular economic models, and the relationship between the circular economy and new technologies. The development and use of alternative construction materials in the building and construction industry are at the forefront of current literature [63,64]. The use of various types of aggregates, such as solid waste, plastics, foams, and recycled concrete from demolished buildings, as reinforcement materials in cement-based construction composites, asphalt, or geo-polymers can be interpreted in the context of the circular economy [59,65]. This approach aims to promote the recycling of these materials and/or reduce the use of matrix constituents, such as cement and sand, to reduce waste and promote a more sustainable and responsible use of resources. Thus, their use can make a significant contribution to the transition to a circular economy.

Promoting the use of post-industrial waste in the production of thermally enhanced building materials represents a promising approach to reduce the overall cost of the composite, minimize energy consumption, and reduce CO_2 emissions [66–69]. Therefore, there is a growing need to develop new, cost-effective insulation materials for building envelopes [70], with particular emphasis on integrating reinforcing materials into a cement matrix, such as concrete, as shown in Figure 2a [71–77]. The traditional approach to improving the insulation properties of walls is to incorporate the insulation layer into the constructed foundation wall, resulting in increased wall thickness and longer construction time [78]. To address these design deficiencies, several researchers are currently investigating the incorporation of insulating materials into various building components such as plaster [79], concrete [80,81], mortar [40,51,66], and building bricks [82–84]. Fibers are one of the most extensively researched insulation materials for their use in cementitious materials and have proven to be an effective solution for minimizing heat loss. In fact, numerous studies have been carried out in this research area to investigate new cement-based composites reinforced with a variety of fibers, including banana fiber [85], coconut fiber waste [86], wool fiber [87] and Acaï [88], palm fiber [89,90], agricultural fiber waste [73], coconut fiber [77], rice straw fiber [91], recycled brass fiber [92], and basalt fiber [93].

Therefore, converting textile waste into construction materials represents a sustainable approach to reducing the environmental impact of the textile industry [94–96]. Textile fibers in particular can serve as an efficient material for thermal insulation and can effectively reduce heat transfer due to their relatively low thermal conductivity compared to other insulation materials [97]. In Figure 2b, the findings of a bibliometric analysis that visually presents the keyword trends related to “textile fiber waste” can be observed. The clusters in the figure illustrate the connections between textile fiber waste and various related topics such as dyeing, textile treatment, and recycling. This cluster analysis shows that there is limited research focused on studying the effects of integrating textile fibers as thermal reinforcement in cement concrete [98].

Textile Reinforced Mortar (TRM) as a fiber-reinforced cementitious compound is assumed to represent a promising material based on the exceptional characteristics of textile fibers. Based on a literature search, the TRM composites were rated for a limited number of applications. In general, fabric meshes and textile yarn have been employed to enhance the tensile strength, ductility, and durability of cementitious composites [99–108]. Nevertheless, there is a lack of research regarding the use of textile fibers, such as the application of spinning waste as a thermal reinforcing material in cementitious composites. Fabric shavings [109] have been studied by Oliveira et al., for instance, for use in cementitious

mortar. They reported that the fabric yarn reduced the mechanical performance of cement mortar except for the tensile adhesion strength. Moreover, subjecting the fabric yarn mortar to a thermal test at 60 °C reveals a difference of 12 °C between the inner surface and the reference face owing to porosity. Other researchers [98] have evaluated the possibility of incorporating textiles into building applications. The results showed that increasing the textile content increased the thermal stability of the cement mortar. Truong et al. demonstrated the feasibility of using hybrid waste fishing-net textiles and fibers for retrofitting structural concrete, achieving significant strength improvements over non-strengthened concrete, though with lower performance than commercial glass textile composites [110]. Dinh et al. developed sustainable textile-reinforced composites (TRCs,) incorporating lightweight expanded glass aggregates, fly ash, and nylon fibers, revealing optimal material configurations for superior tensile performance and cracking resistance, supported by a predictive analytical model [111]. Fernandes et al. explored the reuse of calcined textile sludge as a supplementary cementitious material, showing enhanced pozzolanic activity, improved compressive strength, and microstructural densification, providing a sustainable solution for industrial waste [112]. Pham et al. studied the effects of dispersed fibers in lightweight carbon TRCs, noting improved tensile behavior and multiple cracking patterns, particularly with shorter fibers, and validated an analytical model for predicting tensile stress–strain responses [113].

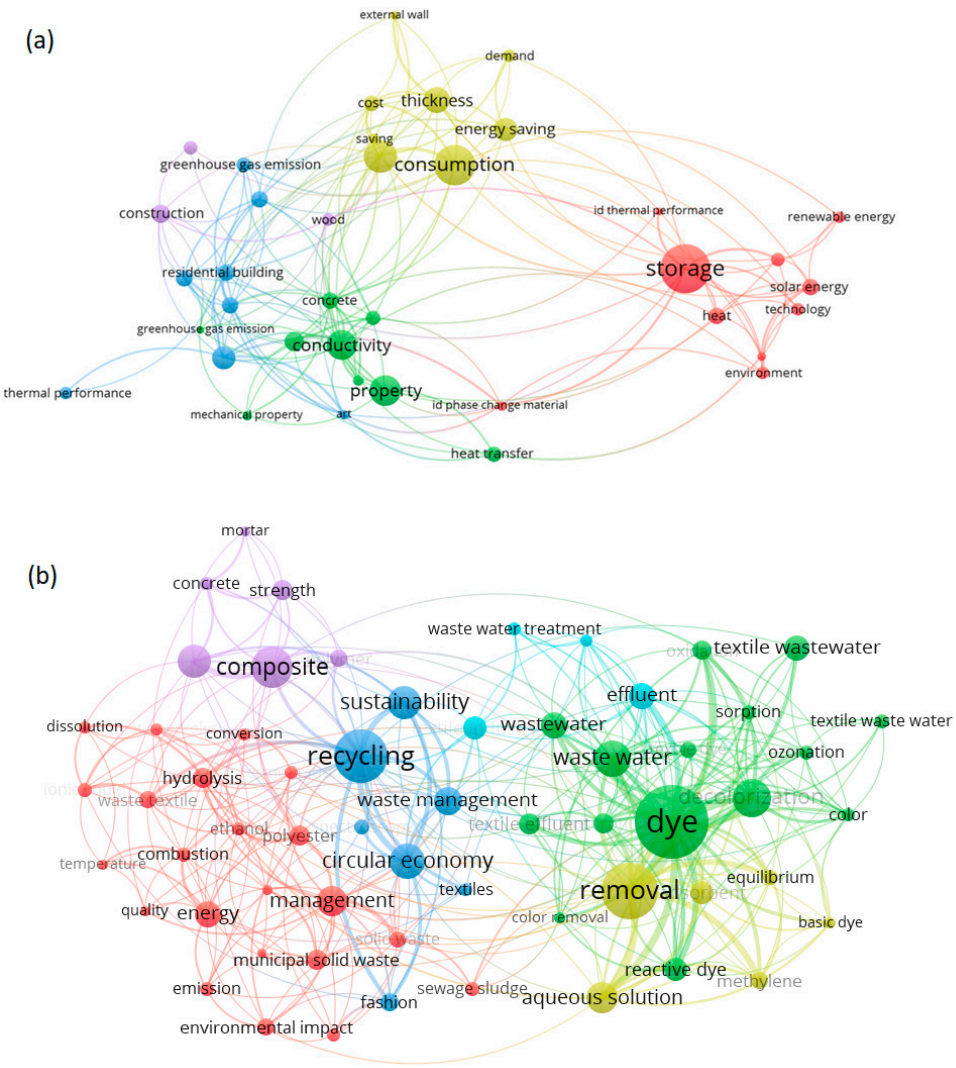


Figure 2. A network visualization of keywords related to (**a**) the thermal insulation of greenhouses; (**b**) textile fiber waste.

Furthermore, several studies have examined the possibility of integrating phase-change materials (PCMs) into construction applications. Zhang et al. [114] optimized the design of PCM-to-air heat exchangers, demonstrating significant energy savings for residential cooling. Dallaire [115] analyzed a dual-stack air–PCM heat exchanger with an innovative airflow design, showcasing its potential to reduce cooling loads effectively. Furthermore, François [116] conducted experimental and numerical studies on PCM-integrated roofing systems, demonstrating improved thermal performance by mitigating overheating. This work highlights the effectiveness of PCM-based technologies as alternative solutions to summer cooling challenges. To this end, this study aims to develop a new building material with low thermal conductivity by incorporating two types of textile waste into cement-based mortars. Several textile fiber-reinforced composites were made by replacing volume fractions of the mortar sand with different percentages of fiber waste. The reinforced mortars produced were characterized mechanically and thermally. Moreover, a numerical study using COMSOL Multiphysics was conducted to investigate the effect of incorporating these thermally reinforced mortars to address building cooling challenges in summer conditions. The optimization of the room structure was guided by an assessment of the air-temperature fluctuations. Overall, this study highlights the crucial role of incorporating fiber waste into construction materials, which not only improves their thermal and mechanical properties but also makes a significant contribution to energy-efficient building solutions. This approach represents a significant advancement in textile-reinforced mortars by integrating textile fiber waste to enhance both the thermal and mechanical properties of building materials, contributing to sustainable and energy-efficient construction solutions. By developing computational models using COMSOL Multiphysics, the study accurately predicts thermal properties and introduces the innovative use of phase-change materials (PCMs) to optimize building cooling systems under extreme summer conditions (Figure 3).

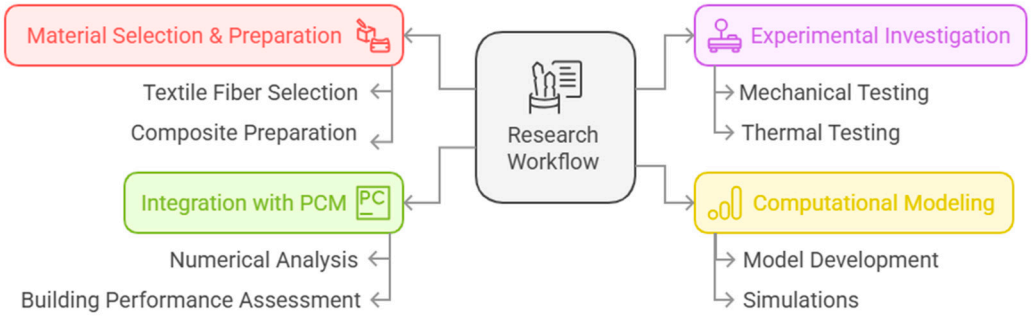


Figure 3. A schematic diagram of the research methodology.

2. Sample Preparation

To produce the cementitious mortars, Portland cement, according to the EN-197-1 standard [117], was used as a binding agent and natural sand as a fine aggregate. Two distinct types of textile waste were also utilized as reinforcing materials. Type I textile fibers (TF_I) included a variety of fibers, including those derived from materials such as linen, cotton, and polyester. These fibers were selected for their special characteristics and their combination provided a diverse reinforcing component. On the other hand, Type II textile fibers (TF_II) include exclusively cotton fibers, offering a more homogeneous and unique fiber composition. This dichotomy between textile types enabled a comparative analysis of how the diversity of materials within Type I, compared to the uniformity of Type II, influenced the performance and characteristics of textile-reinforced composites. Table 1 provides a comprehensive overview of the thermal characteristics of the textile fibers used in this study along with the other mortar components.

Table 1. Thermal properties of textile-reinforced mortar components [69].

Materials	Thermal Conductivity [W/m·K]	Thermal Diffusivity [mm^2/s]	Volumetric Heat Capacity [MJ/m^3·K]
Cement	0.140	0.201	0.694
Sand	0.335	0.278	0.278
TF_I	0.082	0.418	0.196
TF_II	0.070	0.320	0.200

Before the two types of textile fibers were added to the mixture, they were injected with compressed air. This step was crucial to ensure the uniform distribution of the textile fibers throughout the mortar mixture. The mortar mixes were manufactured with a cement-to-sand volume ratio of 1:4. By replacing some of the sand in the mortar mix, cementitious composites reinforced with textile fibers were produced. In this substitution, volume fractions of textile fibers were incorporated in four different amounts: 10%, 20%, 30%, and 40%. Figure 4 depicts the precise mix composition for all mortar mixes. All mixing procedures were carried out using a mechanical mixer, following the guidelines specified in the standard EN 1015-2 [118]. Then, the prepared slurry was carefully poured into molds measuring 40 × 40 × 160 mm, as shown in Figure 5. The molds were then subjected to a drying period of 24 h at a controlled temperature of 20 °C, allowing for the initial setting and hardening of the samples. After the air-drying phase and the removal of the molds, part of the samples were immersed in water for 7 days, while the rest were left in water for an extended curing period of 28 days. These different curing conditions were established to examine the effects of short- and long-term water exposure on sample properties.

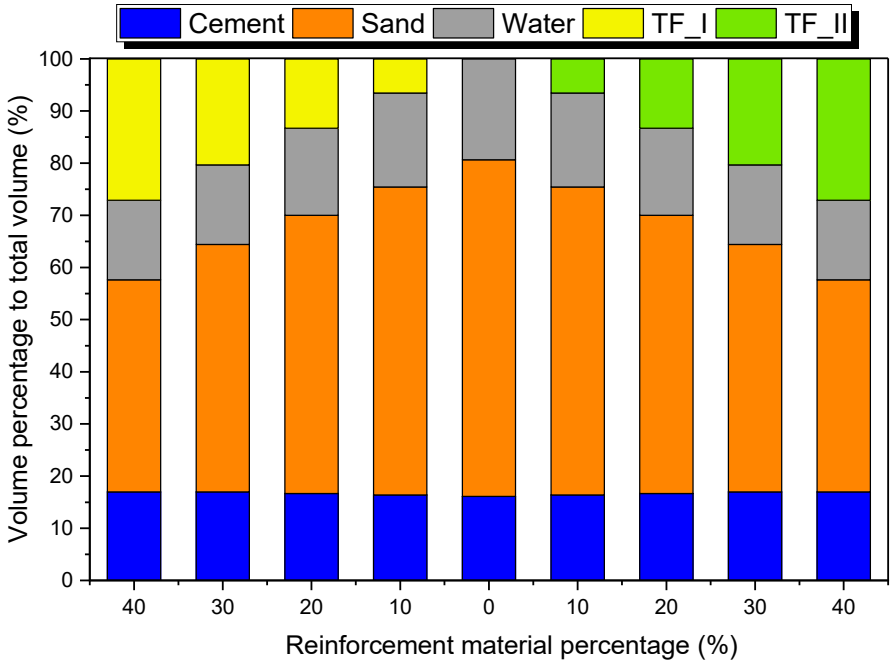


Figure 4. Formulation of the composite material with reinforced materials.



Figure 5. (**a**) TF_I-, (**b**) TF_II-, and (**c**) textile-reinforced mortars after water curing.

3. Characterization of Samples

3.1. Assessment of Workability and Density

To thoroughly evaluate the properties of the mixtures, the workability and density of each mixture were evaluated. This analysis focused on both the fresh and hardened states of the materials. A flow table test was carried out to assess the workability of the mixtures according to the nomenclature described in the European standard EN 1015-3 [119]. This test allows us to accurately evaluate the extent to which mixtures can be manipulated and shaped in the earliest stages of the construction process. On the other hand, bulk density is a crucial parameter that can significantly influence the performance of construction materials. To comprehensively evaluate the bulk density, tests were conducted in both fresh and cured states. These tests comply with the European standards EN 1015-6 [120] and EN 1015-10 [121], respectively.

3.2. Mechanical Evaluation

To analyze the mechanical properties of cured cementitious composites, a mechanical characterization was performed. This assessment required the performance of flexural and compressive strength tests, following the guidelines of the EN 1015-11 standard [122]. These tests were performed using a mechanical testing machine with a double-head, as shown in Figure 6a. This machine provided precise and controlled testing conditions. The evaluation began with a three-point bending test in which each sample was subjected to a controlled loading rate of 50 $\pm$ 10 N/s. This test allowed us to evaluate the material resistance to bending forces, providing valuable information about its flexibility and resistance to deformation. Subsequently, one of the two fragments from the bending test was chosen for the compressive strength test, which was carried out at a loading rate of 2400 $\pm$ 200 N/s. This test allowed us to determine the material ability to resist compressive forces and its overall resistance under pressure. The tests were carried out until the specimen reached its breaking point, and the recorded breaking load provided essential data about the structural integrity of the material and its ability to withstand stress. Then, the mechanical strengths of all cementitious mortars were determined using mathematical expressions.

For maximum flexural strength S_f estimation, the following equation is utilized:

$$S_f = (3F_{max}L) \ / \ (2\ b\ d^2) \quad (1)$$

where F_{max} is the maximum load exerted during the bending test, L denotes the span length between support points, while b and d correspond to the width and depth of the sample, respectively.

Similarly, the compressive strength S_c can be ascertained employing the subsequent equation:

$$S_c = F_{max} / A \quad (2)$$

In this context, F_{max} stands for the maximum load experienced during the compression test, and A represents the cross-sectional area of the sample.



Figure 6. Thermal and mechanical machines in the GREiA research center, Spain: (**a**) mechanical testing machine; and (**b**) analyzer of thermal properties.

3.3. Thermal Evaluation

For the thermal characterization of the samples, an analyzer of thermal properties, as shown in Figure 6b, was used. This particular instrument works on the principle of a transient linear heat-source method to evaluate the thermal conductivity. The key element of this setup is the probe, a sophisticated device that combines a needle equipped with an integrated heating element and a temperature sensor. This dual functionality is crucial for capturing the complex dynamics of the thermal conductivity of the samples. First, the second residual fragment obtained from the bending test was perforated using a hammer drill. A key preparatory measure was used to thoroughly clean the hole in each sample with compressed air and then fill these dimples with thermal paste. This step ensured an optimal thermal interface for accurate readings. The process begins with an activation of the heating element, which is achieved by passing an electric current through it. This activation initiates the complex interaction of heat transfer within the material. At the same time, the system records the temporal evolution of the sensor temperature, providing insight about how the material reacts to different heat inputs. All the samples were placed in a controlled climatic chamber during the data collection. The temperature was meticulously maintained at approximately 20 °C to ensure the consistency and accuracy of the measurements. The evaluation of the experimentally determined thermal conductivity involves a rigorous analytical comparison process. This comparison involves the use of various models, namely the series and parallel model [123–125], the Maxwell model [124], the Rayleigh model [126], the Hashin and Shtrikman model [123], the Hatta and Taya model [123,127,128], and the Nielsen and Lewis model [129–131]. These models rely on a set of equations thoughtfully organized in Figure 7.

Since the analyzer of thermal properties does not provide all the thermal properties of a sample, a numerical model developed with COMSOL Multiphysics software was used to predict the thermal diffusivity and volumetric heat capacity of textile-reinforced mortars.

A comprehensive three-dimensional model was developed consisting of a rectangular block defining the matrix of the mortar. Within this block, spherical units were inserted to represent the reinforcing material. To tackle the thermal properties, the simulation focused on a steady-state heat-conduction scenario and was based on several key assumptions:

- Heat transfer was confined solely to the x-axis.

- Surfaces perpendicular to the heat-flow direction were assumed to be isothermal. Specifically, one surface was set at a fixed temperature of 15 °C, while the other surface was maintained at 40 °C.
- All other surfaces parallel to the *x*-axis were treated as adiabatic, meaning that no heat exchange occurred through these surfaces.

The model accuracy was verified by comparing the predicted thermal conductivities with the experimental results. After validating the model, it was then employed to calculate the thermal diffusivity and volumetric heat capacity for all the samples.

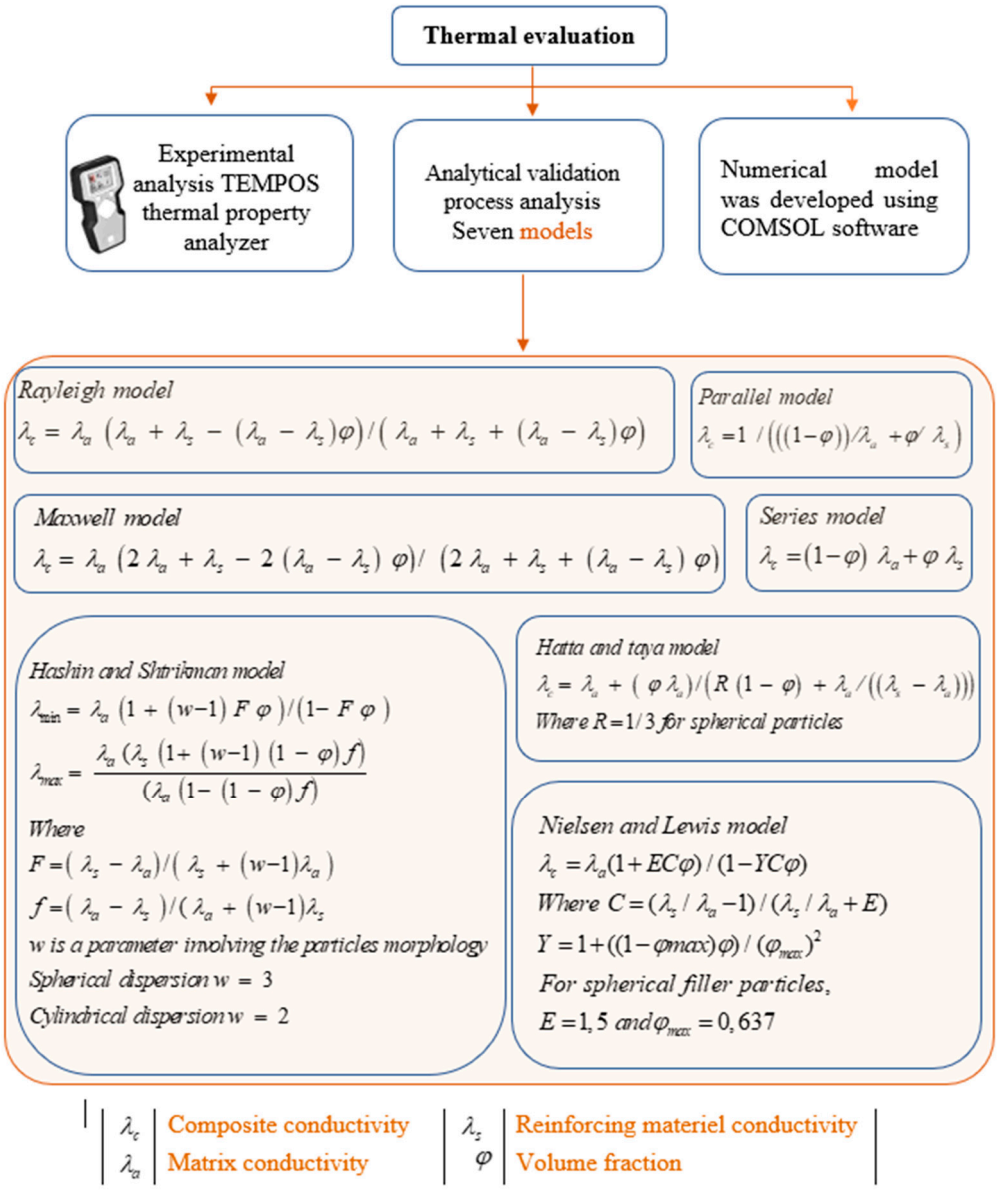


Figure 7. Thermal analysis of reinforced-mortar composites.

4. Modeling the Impact of Integrating Textile-Reinforced Composites

This section is dedicated to the numerical modeling of the combined effects of textile-reinforced mortar and phase-change material (PCM) microcapsules (DS5001X: Microtek Labs, Dayton, OH, USA) on the thermal performance of a building structure, particularly in summer conditions. The modeling is conducted using the COMSOL software. This numerical investigation conducted upon a previous experimental study performed within a 1-m^3 cabin, as shown in Figure 8a, located at the Research and Technology Center of Energy

(CRTEn) at Borj Cedria, Tunisia. The cabin is constructed primarily with brick walls, with both sides covered by a 20 mm thick layer of cement mortar. The roof, on the other hand, consists of a 100 mm thick concrete layer. The methodology followed in this section involves altering the roof and the wall configurations to assess the impact of various materials. The assessment of the thermal environment within this segment involved the development of a 3D geometry, considering the transient nature of the problem. The study incorporated the key aspects of heat transfer, phase-change material characteristics, and laminar flow characteristics to comprehensively analyze the transient temperature distribution in the 3D structure. Furthermore, the influence of solar radiation on temperature variations was accounted for by employing the surface-to-surface radiation module within COMSOL. The model also considered the actual location of the reference room in Borj Cedria, Tunisia, ensuring it was exposed to the same meteorological and boundary conditions, including heat convection on its surfaces. The study also explored the impact of variations in room configuration by evaluating changes in air temperature of the room, as indicated in Figure 8b,c. This comprehensive investigation aims to provide valuable insights into how these combined materials and configurations affect the thermal performance of building enclosures, particularly in hot weather conditions. The thermal properties of the used materials are given in Table 2.

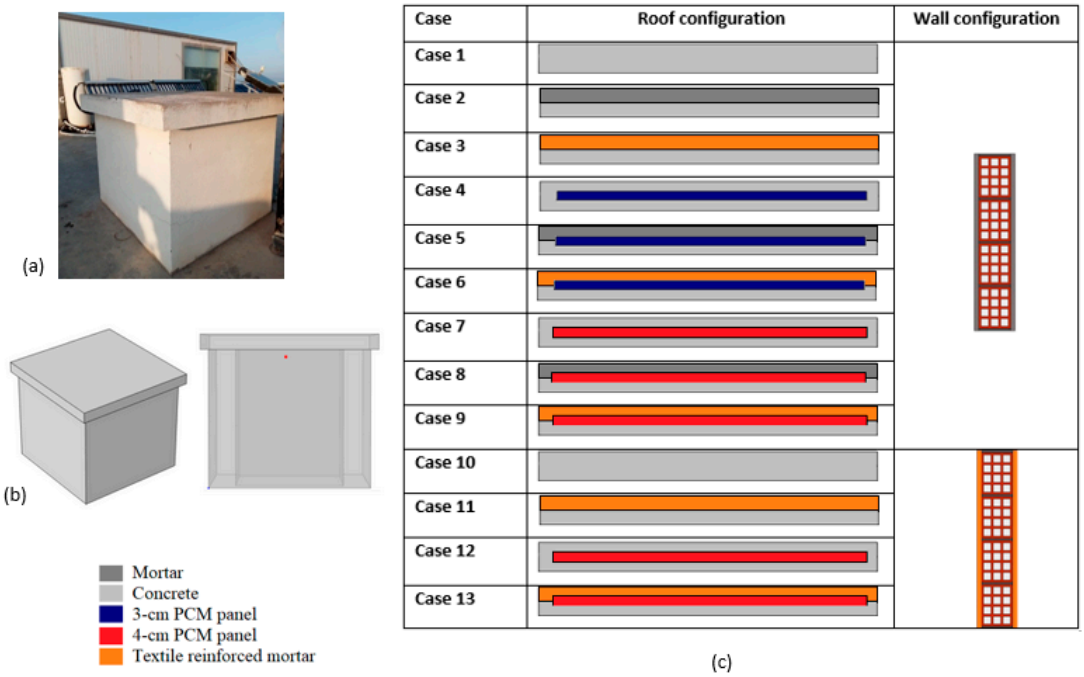


Figure 8. (**a**) Experimental room; (**b**) 3D geometry designed with COMSOL; and (**c**) studied configurations.

Table 2. The thermal properties of the used materials.

Material	PCM DS5001X	Concrete
Thermal conductivity of solid [W/m·K]	0.2	1.8
Thermal conductivity of liquid [W/m·K]	0.13	-
Specific heat capacity of solid [J/kg·K]	1700	880
Specific heat capacity of liquid [J/kg·K]	2153	-
Latent heat [kJ/kg]	130	-
Density [kg/m^3]	995	2300

5. Analysis of Physico-Thermo-Mechanical Properties of Developed Composites

5.1. Workability and Density Results

The amount of water added to the dry mix was adjusted differently for each textile type and fiber content to achieve acceptable workability. The changed proportions of the cement mortar mixture are summarized in Figure 4. The water–cement ratio (W/C) values for different fiber contents are shown in Figure 9. The measured flow diameter of the control mixture (CM) was 145 mm. In this test program, the flow diameter of all mortar mixes was maintained at a specified value of 145 ± 5 mm to achieve a fluid and usable consistency. It can be observed that the water requirement of fiber mortars was significantly higher than that of normal mortars. For mixtures with the same fiber content but different textile types, TF_II-reinforced mortars showed a higher water requirement to achieve the same workability than TF_I mortars. This may be related to the different nature of the TF_I and TF_II fibers. Despite the higher water requirement, the addition of higher textile contents slightly reduced the workability. For the lower percentages of 10% for both TF_I and TF_II, the water-to-cement ratio (W/C) remained constant at 1.2. However, at higher reinforcement levels of 30% and 40%, the W/C ratio was optimized and increased to 1.45. Interestingly, when higher proportions of TF_I were added to the cement mixture, a reduction in the W/C ratio to 0.1 was observed compared to TF_II at the same percentage. It is noteworthy that these fibers display exceptional water absorption, emphasizing the importance of the careful selection of the water–cement ratio.

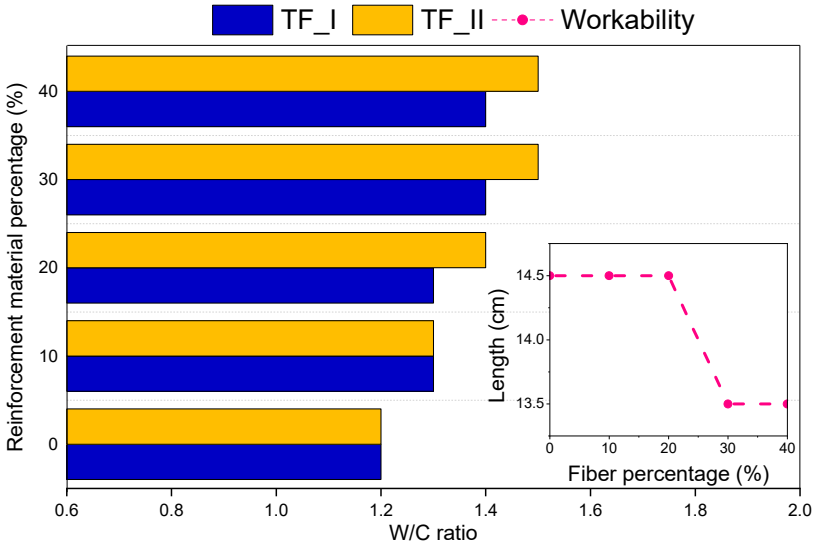
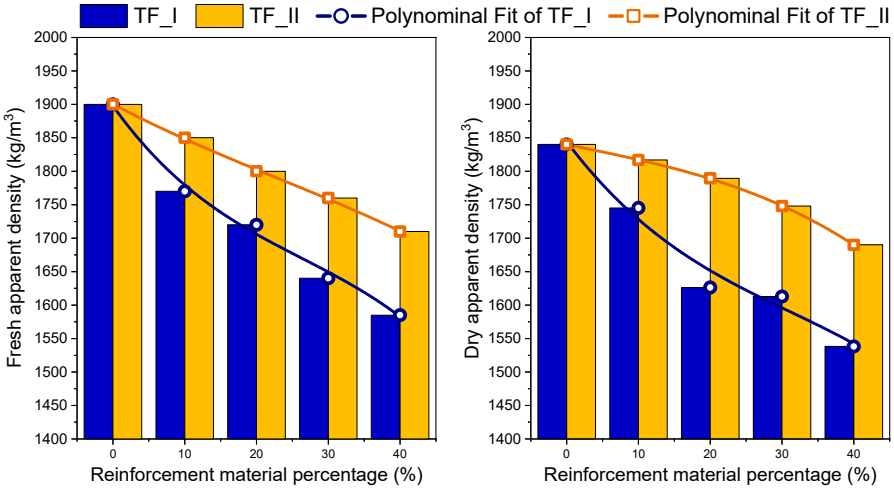


Figure 9. Workability testing of two types of textile-reinforced mortars.

Figure 10 illustrates the variation in density of the samples in both the fresh and dry states. The control cement mortar (CM) had the highest density in both the fresh and dry states, recording a value of 1900 kg/m^3 and 1840 kg/m^3, respectively. For TF_I mortars, as the percentage of reinforcement material increases, the fresh density shows a decreasing trend. At a replacement rate of 10%, the density drops to 1653 kg/m^3, and it continues to decrease progressively to 1620 kg/m^3, 1540 kg/m^3, and 1485 kg/m^3 with percentages of 20%, 30% and 40% of fibers. For the dry density, the mortar reinforced with 10% of TF_I fibers shows a value of 1745 kg/m^3 at 10%, and then slightly decreases to 1626 kg/m^3 at 20%, and finally follows a more consistent downward trend and reaches 1538 kg/m^3 at a replacement level of 40%. For the TF_II composites, the fresh density decreases steadily as the proportion of reinforcing material increases, showing a value

of 1.810 kg/m^3, 1.785 kg/m^3, 1.742 kg/m^3 and 1.698 kg/m^3 at a replacement content of 10%, 20%, 30% and 40%, respectively. Concerning the dry density, the TF_II enhanced mortars show a value of 1816 kg/m^3 with a textile content of 10% that decreases for high proportions, reaching a value of 1690 kg/m^3 with a replacement level of 40%. The addition of both TF_I and TF_II fibers to the cement mortar led to a reduction in density. However, the mortars incorporating TF_I fibers show lower densities than those reinforced with TF_II. When compared to the reference mortar, the inclusion of 40% textile resulted in a decrease in dry-state density, with a reduction of approximately 300 kg/m^3 for the TF_I and 150 kg/m^3 for the TF_II. These results illustrate the influence of textile reinforcement on the density of the mortar and show clear differences between the two types of fibers and their respective effects on the material properties. The reduction in density in fiber-reinforced mortars can have practical implications. While lower density generally contributes to improved thermal insulation and reduced weight, which can be advantageous in applications such as energy-efficient buildings or situations requiring lightweight materials, it may also lead to potential drawbacks. One such drawback is the possible reduction in structural stability. A decrease in density could result in lower compressive strength, potentially affecting the overall load-bearing capacity of the mortar. In structural applications, this reduction in stability may require careful consideration of the material's suitability or the need for additional reinforcement to ensure performance requirements are met without compromising safety or durability.



Equation	y= Intercept + B1*x^1 + B2*x^2 + B3*x^3			
Plot	Fresh apparent density		Dry apparent density	
	TF_I	TF_II	TF_I	TF_II
Intercept	1898 ± 19.5799	1900 ± 3.5599	1844 ± 35.2104	1839.94 ± 0.9462
B1	−14.9702 ± 4.981	−5.702 ± 0.9056	−14.2107 ± 8.9571	−2.2052 ± 0.2407
B2	0.3607 ± 0.3162	0.0571 ± 0.0575	0.2910 ± 0.5687	0.0034 ± 0.0152
B3	−0.0046 ± 0.0052	−0.0008 ± 0.0009	−0.0031 ± 0.0094	−0.0011 ± 0.0003
R^2	0.9935	0.9994	0.978	0.9999

Figure 10. Density of two types of textile mortars in fresh and dry states.

5.2. Mechanical Characterization

Coating mortars must possess sufficient mechanical strength to withstand the multiple impacts they may encounter during their lifespan. Consequently, the mechanical performance of textile waste-reinforced mortars (compressive strength and flexural strength) was studied after 7 and 28 days of curing. Figure 11 illustrates the failure mode of the mortars with textiles during mechanical testing. The examination of curing duration revealed its impact on the interaction between textile fibers and the cementitious matrix. Factors such as hydration progress, fiber–matrix bonding, and potential changes in material

properties over time were thoroughly analyzed. A visual inspection of defective samples showed that increasing the proportion of textile reinforcement did not negatively affect compressive or flexural strength. In fact, samples with higher textile content demonstrated satisfactory performance, with strength levels comparable to the reference mortar. These results indicate that the incorporation of textile fibers not only maintains structural integrity but also enhances the mortar's ability to withstand mechanical stresses. When textile reinforcement is evenly distributed and adequately bonded within the matrix, it positively contributes to overall performance, making it a promising solution for sustainable and durable construction materials.

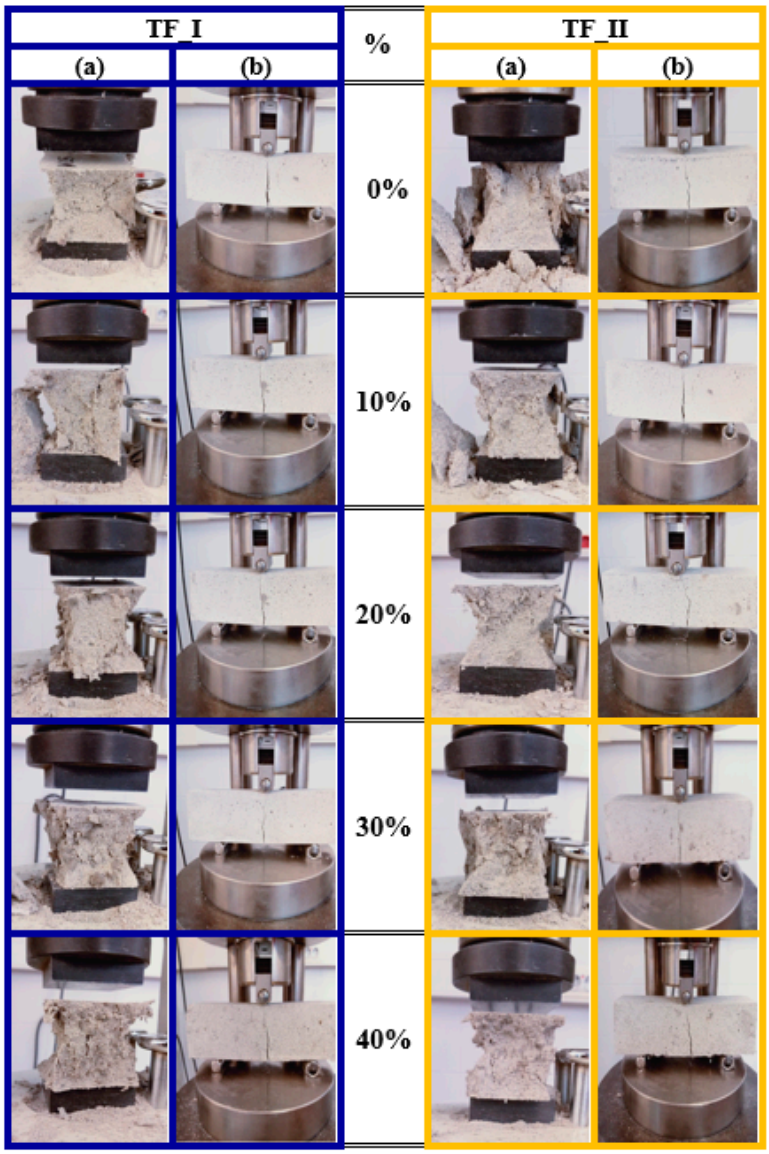
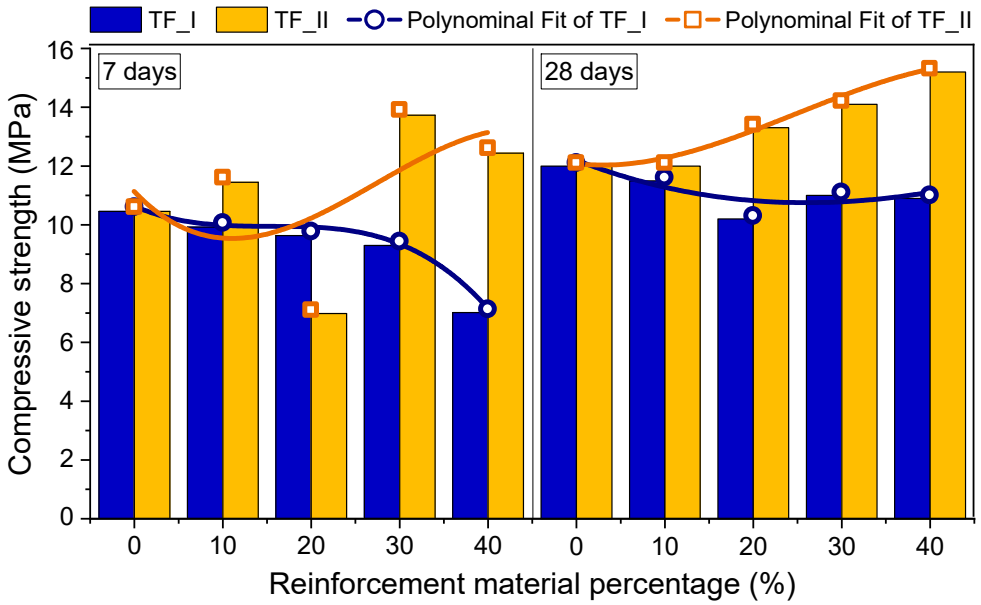


Figure 11. Fracture behavior of textile-reinforced mortars: (**a**) compressive and (**b**) flexural strength.

The results of compressive and flexural strength for all types of mortars after 7 and 28 days of water curing are presented in Figures 12 and 13, respectively. According to the graphs, the mechanical performance of all cementitious mixes improves with the duration of curing. Comparing the compressive strength at the 7th day, the ordinary mortar shows an approximate 13% increase in strength after 28 days of curing. Regarding the bending test, the flexural strength of the control sample increases by 34% between the 7th and 28th days. After 7 days, the mortars reinforced with TF_I fibers show a gradual decrease in compressive strength as the proportion of reinforcing material increases. The values range

from 10.5 MPa for the reference sample to 7.03 MPa for the highest percentage of 40%. Meanwhile, TF_II samples exhibit a lower reduction in compressive strength, reaching a value of 12.5 MPa with a fiber content of 40%.



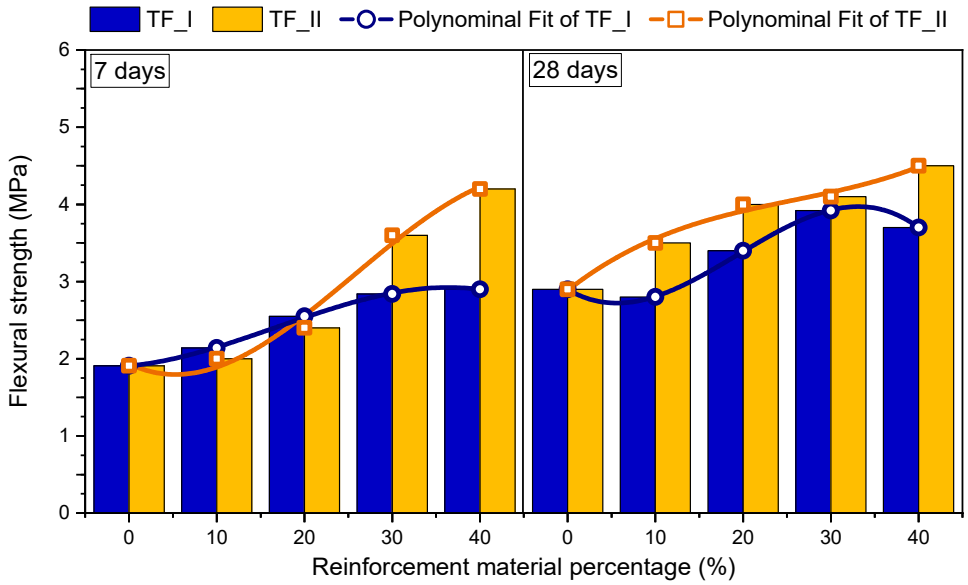
Equation	y= Intercept + B1*x^1 + B2*x^2 + B3*x^3			
Courbe	7-day compressive strength		28-day compressive strength	
	TF_I	TF_II	TF_I	TF_II
Intercept	10.523 ± 0.1911	11.0171 ± 4.2957	12.0843 ± 0.7001	11.9629 ± 0.3085
B1	−0.1321 ± 0.0486	−0.3148 ± 1.0928	−0.1170 ± 0.1781	−0.0352 ± 0.0785
B2	0.0085 ± 0.0031	0.0178 ± 0.0694	0.0026 ± 0.0113	0.0062 ± 0.0050
B3	−0.0002 ± 0.00005	−0.0002 ± 0.0011	−0.00001 ± 0.0002	−0.0001 ± 0.00008
R^2	0.9948	0.2955	0.728	0.9873

Figure 12. Compressive strength of mortars reinforced with textile waste after 7 and 28 days of water curing.

However, when the curing time was extended to 28 days, the control mortar showed an increase in compressive strength, with a difference of 14% compared to the 7-day compressive strength. The TF_I and TF_II mortars show a similar trend with a steady increase in compressive strength, with a difference of 55% (40% of TF_I) and 22% (40% of TF_II), compared to the 7-day compressive strength. These results highlight the importance of curing time and the specific textile reinforcement type, with TF_II outperforming TF_I in terms of compressive strength. In particular, Figure 12 shows that the TF_II in cement mortar leads to a slight increase in compressive strength compared to conventional mortar. For the mixture with 40% TF_II, the compressive strength increases by 16% on the 7th day, while on the 28th day a significant increase in the compressive strength of 21% is observed compared to the mixture without textiles. The results of the mechanical compression tests show that both types of fibers have superior mechanical performance compared to expanded polystyrene and other materials found in the literature such as rice husk ash [38], synthetic plant sponges [42], and ground rubber [132]. These findings provide valuable insights for builders and engineers seeking to optimize their materials and construction processes for improved structural integrity.

Figure 13 provides a comprehensive overview of the bending test results for all fiber-reinforced cement composites. Similarly to the trends observed in compressive strength, mortars reinforced with Type II textiles show better mechanical performance compared to mortars reinforced with Type I textiles after both 7 and 28 days of curing. However, a notable finding is that increasing the proportion of both fiber types continuously increases

the flexural strength regardless of the curing time. After 7 days of curing, the flexural strength experiences an increase, with an improvement of about 34% and 55% for the mortar containing 40% TF_I and the mortar containing 40% TF_II, respectively, compared to the control sample. This highlights the important role that fiber types and their proportions play in improving flexural strength. After a 28-day curing period, the results remain positive, with an increase of approximately 22% for the sample with 40% TF_I and a notable increase of 36% for the sample with TF_II, both compared to the regular sample. Comparing the flexural strength of TF_I- and TF_II-reinforced mortars after 7 and 28 days of water curing, we observe clear patterns in their mechanical performance. After 7 days of curing, the flexural strength of TF_I shows an upward trend with increasing proportion of reinforcing material, ranging from 1.91 MPa (0%) to 2.899 MPa (40%). In contrast, TF_II has varying flexural strength in different percentages, ranging from 1.91 MPa (0%) to 4.2 MPa (30%).



Equation	y= Intercept + B1*x^1 + B2*x^2 + B3*x^3			
Plot	7-day flexural strength		28-day flexural strength	
	TF_I	TF_II	TF_I	TF_II
Intercept	1.9073 ± 0.02243	1.937 ± 0.22428	2.89829 ± 0.01424	2.88571 ± 0.11867
B1	0.01053 ± 0.00571	−0.05542 ± 0.05705	−0.06686 ± 0.0036	0.08952 ± 0.03019
B2	0.00172 ± 0.0004	0.00585 ± 0.00362	0.00697 ± 0.0002	−0.00257 ± 0.0019
B3	−0.0003 ± 0.00000	−0.0001 ± 0.00005	−0.0001 ± 0.000003	0.00003 ± 0.00003
R^2	0.99932	0.98782	0.99978	0.9906

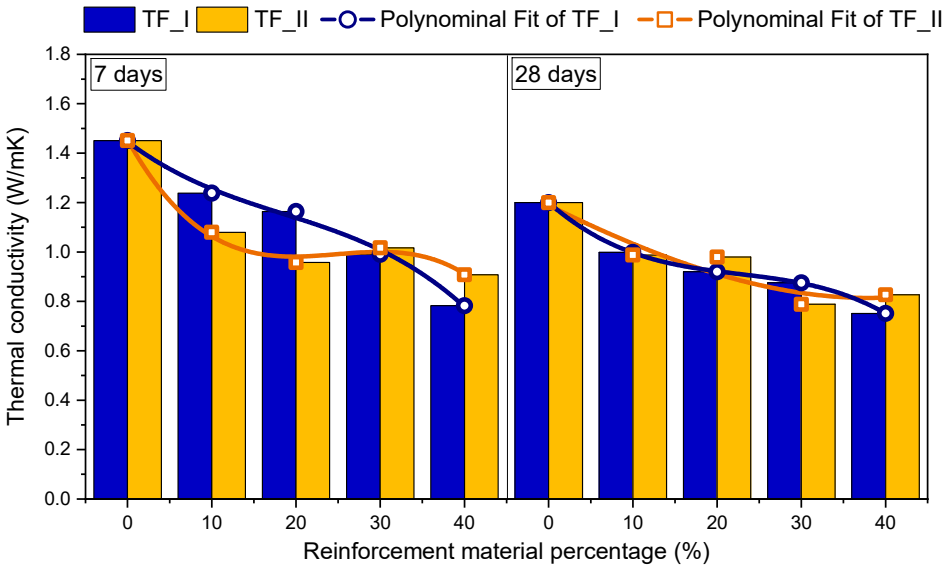
Figure 13. Flexural strength of mortars reinforced with textile waste after 7 and 28 days of water curing.

As the curing period extends to 28 days, TF_I reinforcement continues to demonstrate an increase in flexural strength, with values ranging from 1.9 MPa (0%) to 3.7 MPa (40%). Likewise, TF_II reinforcement exhibits a consistent rise in flexural strength, ranging from 2.9 MPa (0%) to 4.5 MPa (40%).

5.3. Thermal Characterization

Figure 14 provides a comprehensive overview of the thermal conductivity data for textile-reinforced composites after 7 and 28 days of curing. Notably, the impact of varying textile percentages on thermal conductivity is quite pronounced. Across both TF_I and TF_II composites, as the proportion of reinforcement material increases, there is a consistent decrease in thermal conductivity. The 40% reinforced mix of each grade had the lowest thermal conductivity of all mortars of the same grade. Comparing ordinary mortar and

composite reinforced with 40% TF_II, a decrease in thermal conductivity is observed on day 7 with an increasing addition of fibers, reaching a difference of about 46%. Furthermore, the mortar reinforced with 10% TF_II shows a greater decrease in thermal conductivity on day 7 compared to the sample with 10% TF_I, reaching a value of 1.08 W/m K. The results of incorporating TF_II from 10% to 40% show a slightly reduced thermal conductivity, with a difference of 16%. Regarding thermal conductivity after 28 days, both types of textiles show a similar result, reaching values of 0.75 W/m K and 0.8 W/m K for mortar with 40% TF_I and mortar with 40% TF_II. The influence of short- vs. long-term curing conditions on thermal properties is significant, as the curing duration impacts the development of the material microstructure and, consequently, its thermal performance. Longer curing periods allow for a more complete hydration process, enhancing the bond between the cementitious matrix and the textile fibers, thereby improving the insulation properties of the composite. This suggests that both short and long-term curing conditions can effectively enhance the thermal insulation properties of textile-reinforced mortars, with long-term curing providing more stable and improved thermal performance. The addition of textile fibers improves thermal insulation by reducing thermal conductivity, which is consistent with previous research. These fibers not only serve as reinforcing agents for mechanical strength but also reduce the material's density, contributing to better heat resistance. The improvement in thermal conductivity observed with the incorporation of textile fibers emphasizes the importance of fiber content. A higher fiber material content results in greater resistance to heat transfer, thereby improving overall thermal insulation. This relationship between fiber content and thermal performance aligns with previous findings, reinforcing the idea that optimizing the proportion of textile fibers can significantly contribute to energy-efficient building materials.



Equation	y= Intercept + B1*x^1 + B2*x^2 + B3*x^3			
Plot	7-day thermal conductivity		28-day thermal conductivity	
	TF_I	TF_II	TF_I	TF_II
Intercept	1.44653 ± 0.03563	1.45487 ± 0.03363	1.20035 ± 0.00293	1.18857 ± 0.09492
B1	−0.02569 ± 0.00906	−0.06153 ± 0.00856	−0.03014 ± 0.0007	−0.01673 ± 0.02415
B2	0.001 ± 0.0006	0.00259 ± 0.0005	0.00115 ± 0.00005	0.0001 ± 0.00153
B3	−0.00001 ± 0.00001	−0.0003 ± 0.000008	−0.0002 ± 0.0000007	0.000002 ± 0.00003
R^2	0.99496	0.99384	0.99992	0.91355

Figure 14. Thermal conductivity and thermal resistance of mortars reinforced with textile waste.

Figures 15 and 16 provide a graphical representation of the comparison between the experimentally measured thermal conductivities of reinforced mortars by the two types of textile fibers and the values predicted by the analytical models, which are detailed in Section 3.3 and illustrated in Figure 7. These figures offer a visual means to assess the alignment or divergence between the actual data and the model forecasts, facilitating a comprehensive understanding of the thermal behavior of the reinforced mortars. The observed trend in both experimental and theoretical data consistently shows that an increase in the quantity of reinforcing material leads to a decrease in the thermal conductivity of the cementitious mortar. These findings underscore the agreement between the empirical data and the forecasts generated by the series and parallel models, along with the Hashin–Strikman model. This alignment between experimental results and theoretical predictions emphasizes the reliability of these models in explaining the variations in thermal conductivity as a function of the reinforcing material's concentration. In the context of mortars enhanced with TF_I, Figure 15 clearly illustrates that the Rayleigh model stands out as the most accurate predictor, showing just a 5% deviation from the experimental results. This remarkable concordance can be attributed to the inherent characteristics of the reinforcing materials, which possess a fibrous structure. The fibrous nature of these materials plays a crucial role in establishing a correlation between the Rayleigh model and the observed thermal behaviors. The model's ability to consider the thermal properties of individual fibers within the composite proves highly effective in predicting the overall thermal conductivity of the reinforced mortars. This outcome highlights the importance of recognizing the specific attributes of the reinforcing materials when selecting an appropriate predictive model. These fibers can be seen as resembling cylinders that are distributed throughout the cement matrix. The underlying principles of the Rayleigh model are, in many ways, analogous to this configuration, which helps explain the model's remarkable performance in predicting the thermal behavior of these reinforced mortars. This insight is significant as it highlights the suitability of the Rayleigh model in the context of fiber-reinforced mortars, shedding light on the behavior of such materials in real-world applications.

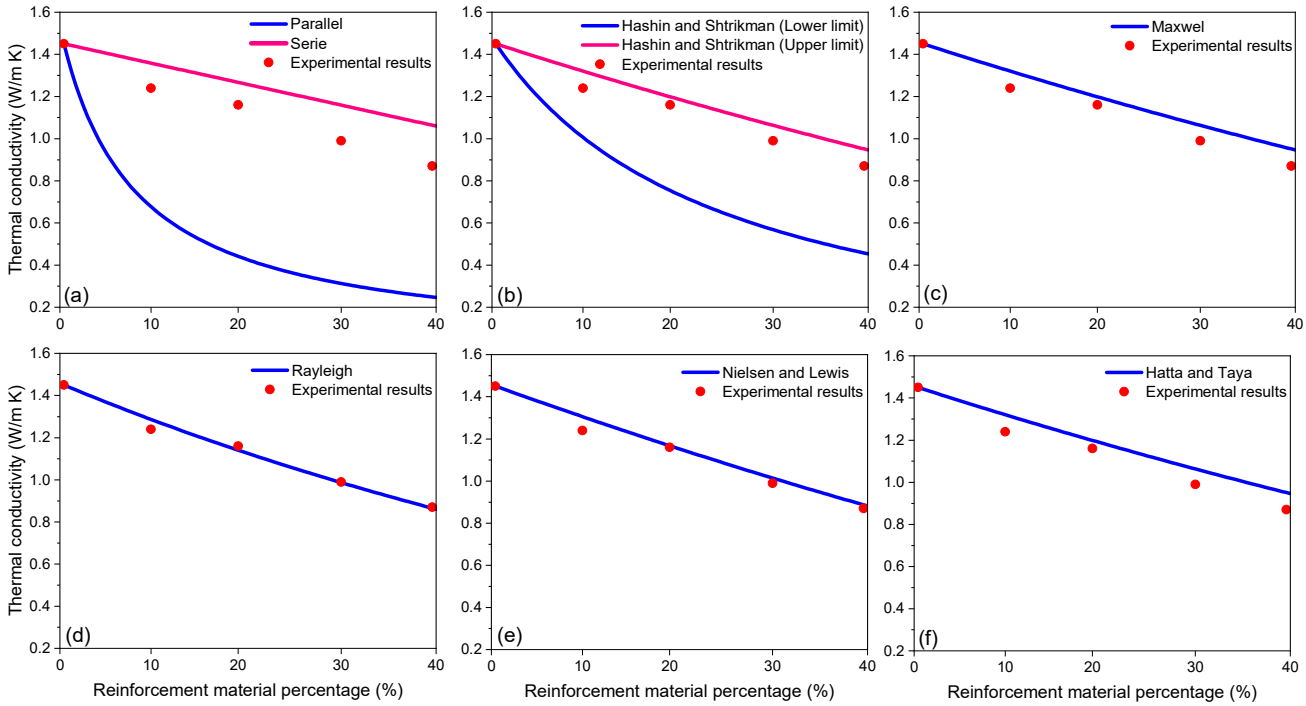


Figure 15. Thermal conductivity of TF_I-reinforced mortars predicted by analytical models: (**a**) Parallel and serie model, (**b**) Hashin-Strikman model, (**c**) Maxwel model, (**d**) Rayleigh model, (**e**) Nielsen-Lewis model and (**f**) Hatta-Taya model in comparison with experimental results.

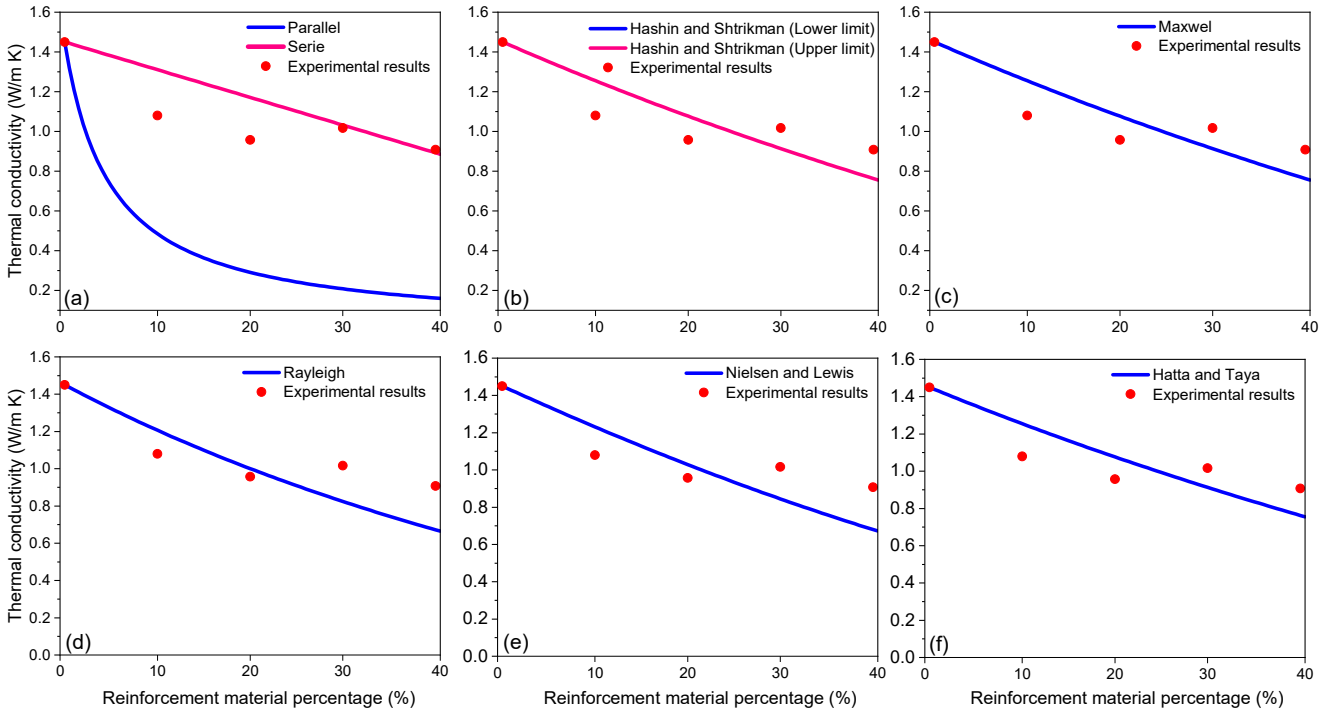


Figure 16. Thermal conductivity of TF_II-reinforced mortars predicted by analytical models: (**a**) Parallel and serie model, (**b**) Hashin-Strikman model, (**c**) Maxwel model, (**d**) Rayleigh model, (**e**) Nielsen-Lewis model and (**f**) Hatta-Taya model in comparison with experimental results.

In the examination of TF_II-reinforced mortars, the insights derived from Figure 16 reveal an interesting pattern. They indicate that the Rayleigh model, while generally effective in predicting the thermal behavior of these fortified mortars, exhibits a slight divergence from the experimental data. This variance is particularly noticeable when dealing with mortars containing lower proportions of reinforcing elements. This discrepancy can be attributed to the Rayleigh model's exclusive focus on the thermal conductivity of the individual materials within the composite. Conversely, when examining samples with higher concentrations of reinforcing materials, the experimental results more closely correspond with the predictions of the serial model. This alignment suggests that the textile fibers were adeptly and uniformly distributed throughout the cement matrix. This even dispersion of fibers within the matrix is a key factor contributing to the enhancement of the mortars' thermal characteristics.

5.4. Estimation of Thermal Diffusivity and Volumetric Heat Capacity of Various Samples

In the quest to ascertain the thermal parameters, including diffusivity and thermal capacity, for the different samples under investigation, we initiate the process with an analytical examination aimed at confirming the experimental results for thermal conductivity, as presented in the preceding section. Following this step, we proceed to develop a numerical COMSOL model, which enables us to derive the diffusivity and thermal capacity values for the samples. This integrated approach ensures a comprehensive understanding of the thermal characteristics of the materials in question. Figure 17 provides a visual representation that allows us to compare the thermal conductivity results of textile fiber-reinforced mortars obtained through numerical simulations with those derived from experimental measurements. This comparative analysis serves to assess the agreement or divergence between the modeled and observed thermal behaviors of these materials, shedding light on their thermal performance and the accuracy of our predictions. This visual representation provides insights into the relationship between the measured and

predicted results, taking into account the textile content of the samples. It underscores a coherent pattern and notes a marginal increase in error for samples with higher textile content. To delve deeper into this observation, it is essential to consider the implications of this error fluctuation and explore potential contributing factors that might elucidate these variations. The thermal conductivity values obtained through experimental measurements consistently appear to be lower than the values predicted by the model. This ongoing discrepancy can be ascribed to various uncontrolled variables that can manifest during the sample preparation process, variables that the model does not account for. These factors encompass elements such as porosity within the material and contact resistance between its components. These observations serve to underscore the resilience and precision of the numerical model. Despite these discrepancies, the model continues to provide valuable insights, emphasizing its overall effectiveness in approximating and understanding the thermal behavior of the materials under study.

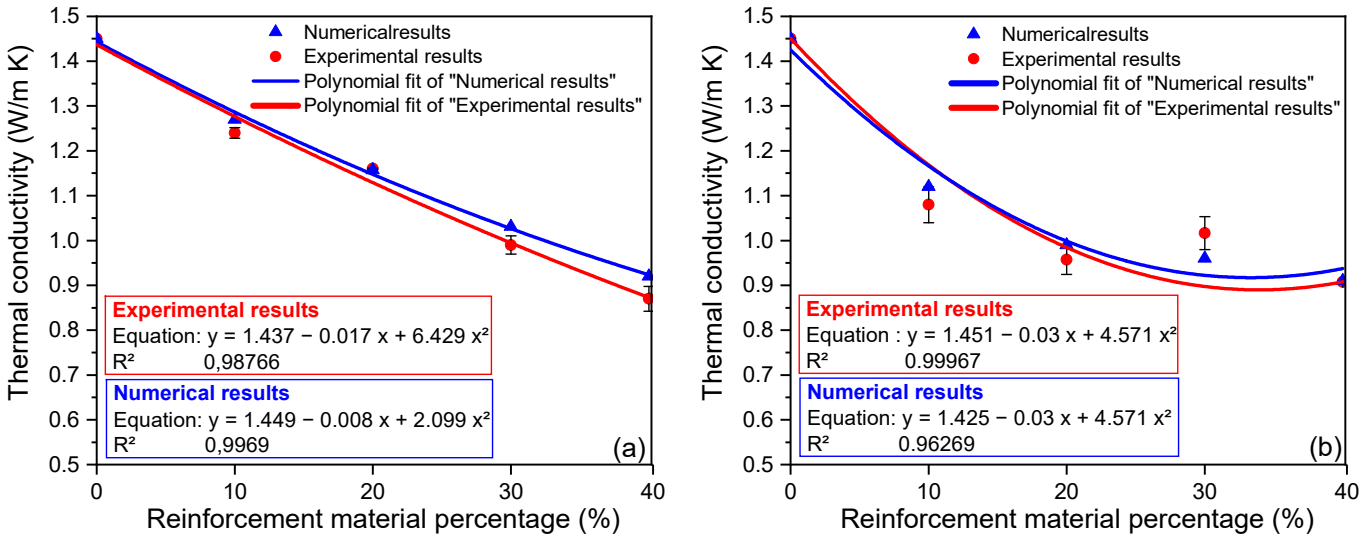


Figure 17. Thermal conductivity of (**a**) TF_I and (**b**) TF_II reinforced mortars predicted by the numerical model in comparison with experimental results.

Figure 18 offers a representation of the numerically predicted thermal diffusivities and volumetric thermal capacities for reinforced mortars, reinforced with TF_I and TF_II. The addition of fibers to the cementitious mortar appears to result in a reduction in both thermal diffusivity and volumetric heat capacity. In the case of low TF_I content, we observe a gradual decline in both thermal diffusivity and volumetric heat capacity for the mortars with textiles. This decline continues until reaching values of 1.13 mm^2/s and 1.12 $MJ/m^3 \cdot K$, respectively. These findings highlight the impact of textile content on the thermal properties of the mortars and provide valuable insights into how different fiber concentrations influence the heat transfer and heat-storage characteristics of the materials. Furthermore, as the proportion of textile fibers is increased to 40%, we observe a notable reduction in both thermal diffusivity and volumetric heat capacity. Specifically, the thermal diffusivity decreases to 0.97 mm^2/s, and the volumetric heat capacity drops to 0.91 $MJ/m^3 \cdot K$. When examining mortars reinforced with 40% TF_II, we similarly observe a decrease in thermal diffusivity and volumetric thermal capacity, reaching values of 1.11 mm^2/s and 1.05 $MJ/m^3 \cdot K$, respectively. The incorporation of textile fiber waste into cementitious mortar consistently leads to reductions in thermal diffusivity and volumetric heat capacity, aligning with the decrease in thermal conductivity. For instance, in comparison to the conventional mortar (CM) sample, where there is a 40% decrease in thermal conductivity for the TF_I sample with (40%), we see a corresponding 21% decrease in thermal diffusivity and a 23% decrease

in volumetric heat capacity. Similarly, in the case of the TF_II sample (40%) with a 37% decrease in thermal conductivity compared to ordinary mortar, we observe a 9% reduction in thermal diffusivity and an 11% reduction in volumetric heat capacity for both TF_I- and TF_II-reinforced mortars. These results highlight the intricate relationship between textile fiber content and the thermal properties of the mortars, demonstrating how varying fiber concentrations can significantly affect heat transfer and heat-storage characteristics.

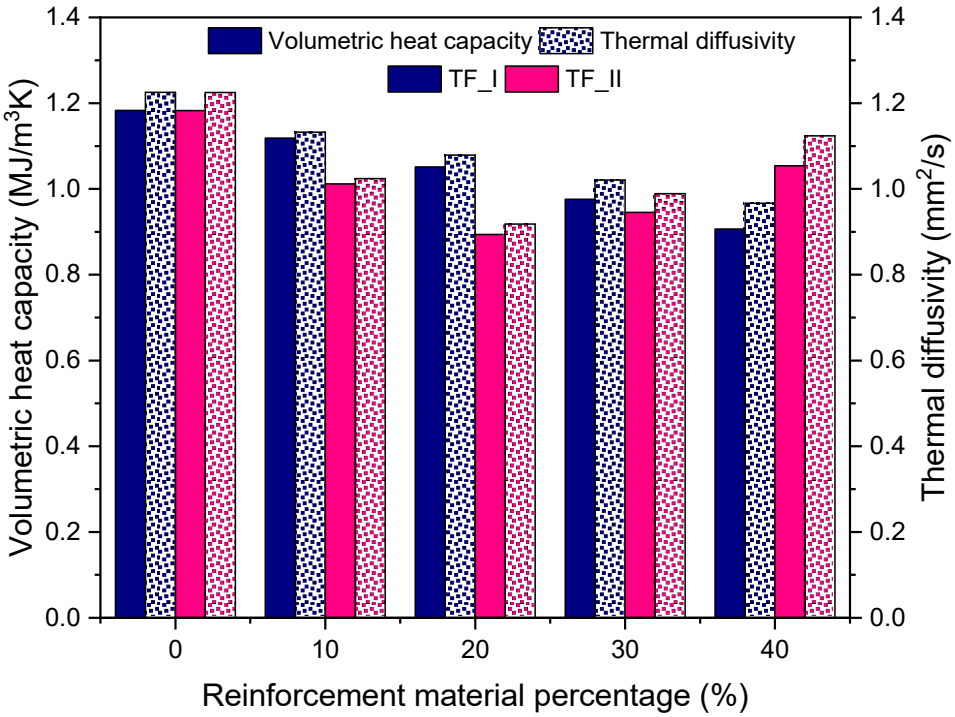


Figure 18. Numerically predicted thermal diffusivity and volumetric heat capacity of textile-reinforced mortars.

5.5. Comparative Analysis of Insulation Materials

Based on the characterization results, the textile-reinforced mortars show a unique balance of thermal, physical, and mechanical properties, making them a promising alternative to traditional cement mortars reinforced with other insulating materials. Table 3 provides a comparison between the current study and previous research documented in the literature. In terms of thermal performance, the addition of the textile fibers significantly decreases the thermal conductivity of cement mortar. The values given are between 0.75 and 1.2 W/mK for textile TF_I and between 0.82 and 1.2 W/mK for textile TF_II. This improvement in thermal conductivity due to the addition of textile fibers is consistent with previous studies that have identified better insulation resistance with the increase in fiber material [74]. In addition, both types of textile fibers improved the thermal performance of cement mortar more effectively compared to other materials such as polymer-coated perlite [133], rubber granulate [132], bagasse or rice husks [45], expanded perlite [134], and expanded polystyrene [50], which is an efficient thermal insulator due to its highly porous and lightweight nature. Although these materials provide excellent thermal insulation, they often exhibit poor mechanical properties such as low compressive and flexural strength, which may limit their applicability in load-bearing or high-stress environments. In contrast, textile fibers not only improve thermal insulation but also improve mechanical performance. Studies have shown that textile fiber reinforcements can significantly improve flexural strength and ductility by improving the post-cracking behavior of cement mortars, thereby providing higher energy absorption and resistance to crack propagation. The results of

the mechanical compression tests show that both types of fibers have superior mechanical performance compared to expanded polystyrene and other materials found in the literature such as rice husk ash [38], synthetic plant sponges [42], and ground rubber [132], which often exhibit brittle behavior and reduced structural capacity. In addition, textile fibers help maintain compressive strength, while other insulation materials often result in a decrease in compressive strength due to their lower density and weaker matrix interactions. Additionally, textile fibers promote sustainability through the use of recycled or waste materials, aligning with the growing importance of green building practices. Overall, textile fiber-reinforced mortars offer a comprehensive solution by combining improved thermal insulation with superior mechanical performance, bridging this gap between energy efficiency and structural integrity. This makes them a sensible alternative to conventional insulation materials, especially in applications that require longevity and resilience in addition to thermal efficiency.

Table 3. Comparative analysis of insulation materials.

Reinforcement Material	Replacement Percentage (%)	Thermal Conductivity (W/m·K)	Flexural Strength (MPa)	Compressive Strength (MPa)	Reference
Expanded polystyrene					[135]
Rice husks					[45]
Expanded perlite					[133]
Juncus acutus					[136]
Human hair					[137]
Sheep wool					[138]
Fiberglass					[103]
Rubber granulate					[132]
Fly ash					[139]
Silica fume					[140]

6. Modeling of Room Integrating Textile-Reinforced Mortar Composites: Case Study

6.1. Climatic Conditions and Model Validation

To validate the accuracy of the numerical model, the variation in air temperature measured in the room was compared with the temperature predicted for Case 1. The validation of this model was carried out on a typical experimental day, as shown in Figure 19a, which provide a detailed overview of the climatic conditions recorded at the experimental site on 17 June 2022. The same meteorological data will be input into the numerical model to predict the thermal behavior of the room in other cases. The fluctuations in the outside temperature and solar radiation are remarkable. The outside temperature is between 33 °C and 22 °C, the average value is 27.7 °C. A significant increase in outside air temperature is observed between 11 a.m. and 3 p.m., while the minimum temperature is recorded between 3 a.m. and 5 a.m. It is worth mentioning that a maximum solar radiation of approx. 960 W/m^2 is measured around midday. Figure 19 billustrates a similar trend between the numerical and experimental values with a root mean square error of 0.48. This consistency of results confirms the reliability of the developed model in predicting heat transfer in the selected room.

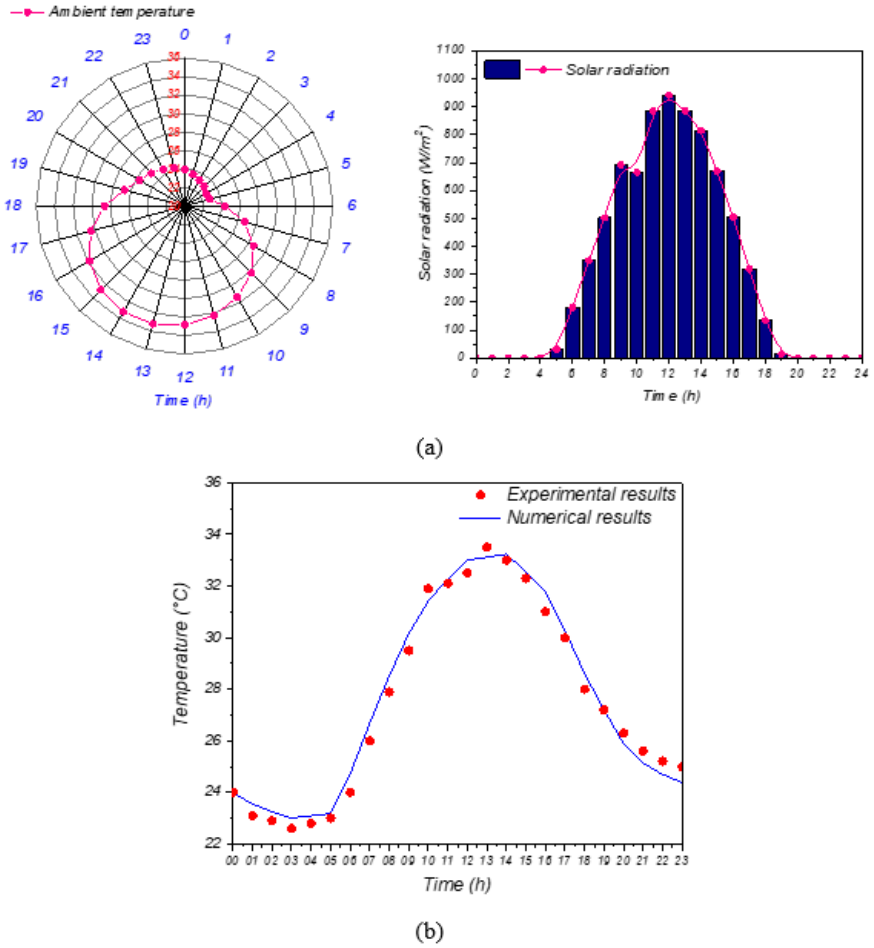


Figure 19. Variations in (**a**) the external air temperature and and the solar radiation at the Borj Cedria site on the day of the experiment and (**b**) a comparison of the experimental and numerical results.

6.2. Evaluation of the Effect of Adding Textile-Reinforced Mortar to a Building's Roof

The simulations consider various scenarios, referred to as Cases 1 to 9, in which modifications are made to the roof while assuming that the cabin walls are constructed using bricks and conventional mortar. This research examines different configurations of roof structures, each with different compositions and integrated materials. In Case 1, the roof is made entirely of concrete. Case 2 represents a roof consisting of a concrete layer on which a layer of standard mortar is applied. In Case 3, the roof comprises a layer of concrete topped with a layer of TF_I-reinforced mortar. Cases 4, 5, and 6 involve a 3 cm thick panel of phase-change material (PCM), which is integrated into the roof structure in different ways. In Case 4, the PCM panel is included directly into a concrete roof, while in Case 5, it is inserted between a layer of concrete and a layer of standard mortar. Case 6 examines a similar structure, but with the PCM board sandwiched between a layer of concrete and a layer of fiber-reinforced mortar. Similarly, Cases 7, 8 and 9 study the installation of a 4 cm thick PCM board in the roof structure: directly in a concrete roof (Case 7), sandwiched between a concrete layer and a standard mortar layer (Case 8), and between a layer of concrete and a layer of fiber-reinforced mortar (Case 9). Figure 20 shows the temperature distribution in each case along a plane perpendicular to the south side of the cabin. The time frame shown is from 6:00 a.m. to 7:00 p.m., with data provided at hourly intervals. Regions with warm and hot temperatures are represented in the visualization by shades of orange and red, respectively. Conversely, colder areas are characterized by blue shades. The profile temperature prominently demonstrates that the integration of a thermally reinforced mortar and a phase-change material into the roof structure mitigates

heat transfer, resulting in a significant reduction in the overall temperature distribution within the cabin. As shown in Figure 20 and the enlargement in Figure 21a at 12 p.m., the reinforced composite material integrated into Case 3 actually acted as a robust barrier to heat transfer and reduced the flow of thermal energy between the indoor and outdoor environments. In addition, Figure 21b, which shows the temperature profile in a plane at the center of the roof, shows that the use of PCM panels helped to reduce heat transfer in the roof. The temperature variation observed when comparing Cases 4 and 7 to Case 1 clearly demonstrates the beneficial effects of integrating phase-change materials. This integration improves thermal regulation by effectively absorbing and releasing thermal energy during phase transitions, thus stabilizing internal temperatures. Furthermore, Cases 6 and 9 clearly show that the inclusion of thermal insulation and PCM in the roof structure leads to the most significant reduction in the temperature profile.

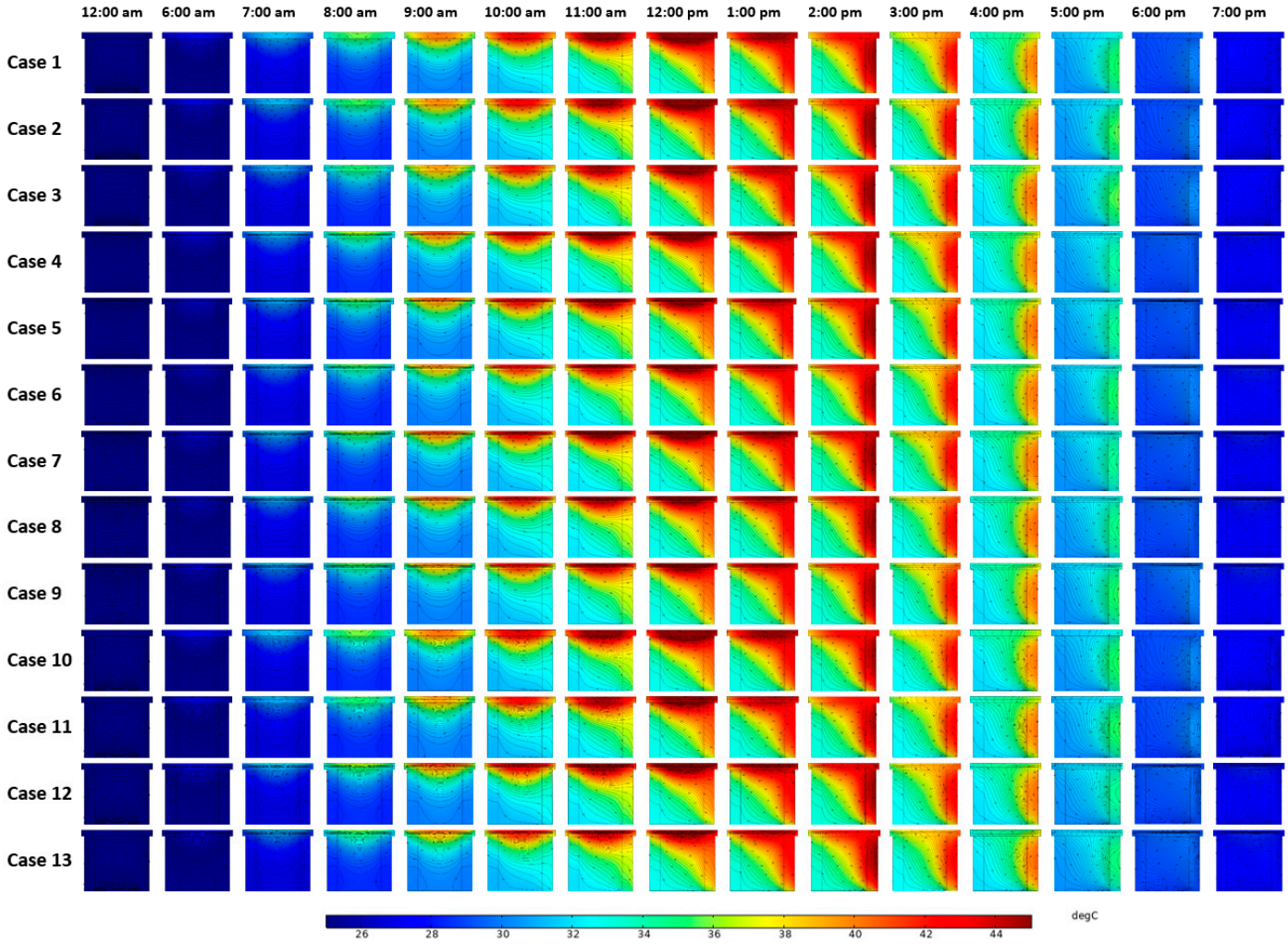


Figure 20. Daily air-temperature profile in each configuration studied inside the cabin.

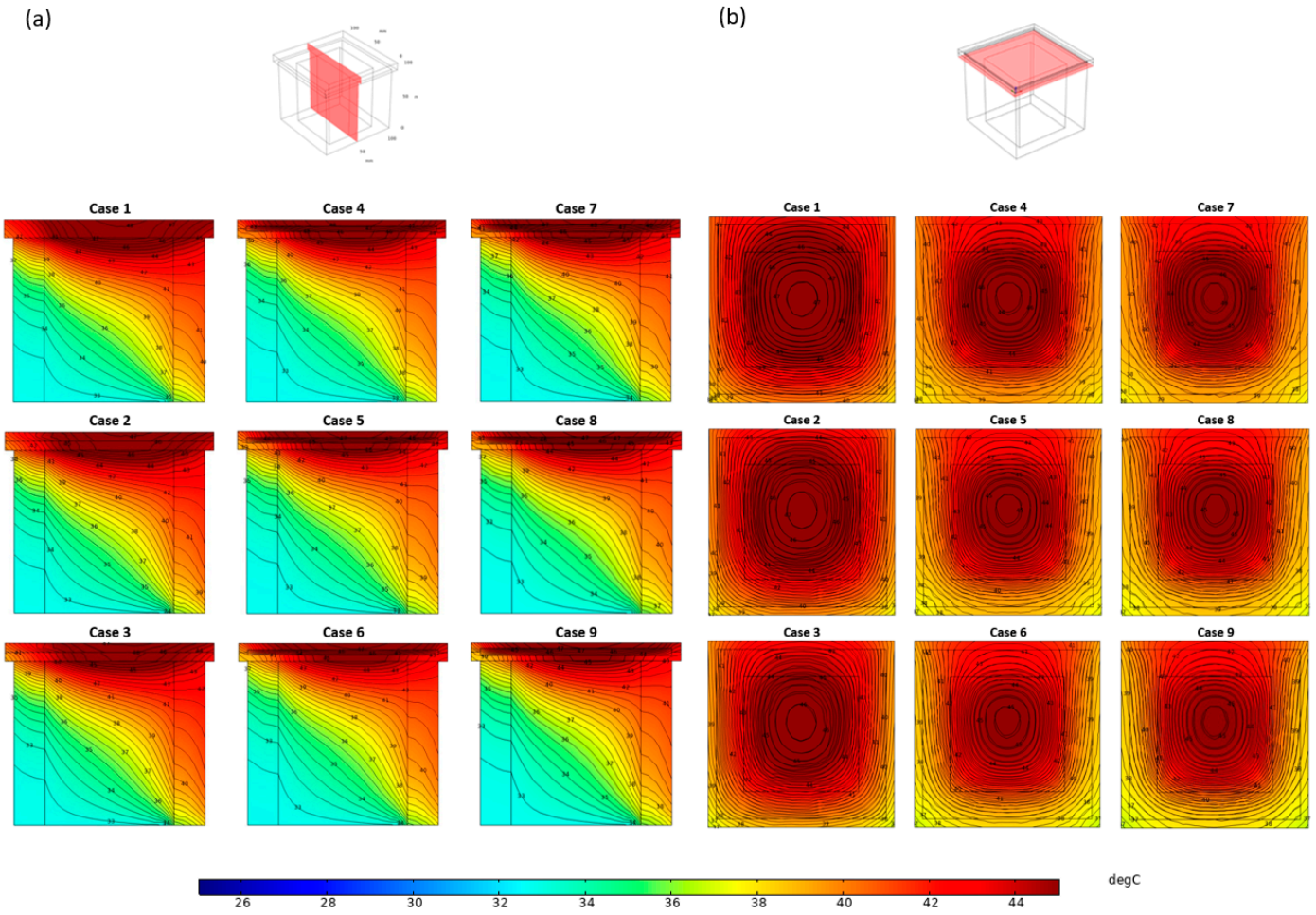


Figure 21. Instantaneous air-temperature profile in the 13 configurations studied: (**a**) transversal cross-section; (**b**) longitudinal cross-section.

Figure 22 shows a comparative analysis of the air-temperature fluctuations between the nine scenarios investigated. Since changes were made in the architectural composition of the roof, the assessment of temperature variations was carried out in close proximity to the roof, as shown in Figure 8b. Figure 22a provides an expanded view of the temperature variation from 10 a.m. to 2 p.m., specifically focusing on the effects of integrating the 40% TF_I-fiber-reinforced composite. As the graphic shows, a temperature of around 45 °C was measured at midday in the cabin with a roof made of 10 cm thick concrete (Case 1). When replacing a 3 cm thick concrete roof layer with a layer of ordinary mortar, there was a temperature drop of 0.5 °C compared to Case 1. Replacing a 3 cm thick concrete roof layer with a layer of ordinary mortar resulted in a temperature drop of 0.5 °C compared to Case 1. An additional temperature reduction occurred when the 3 cm thick concrete roof layer was replaced with a layer of fiber-reinforced mortar, resulting in a temperature decrease of 1 °C compared to Case 1. These results demonstrate the influence of integrating the textile-reinforced mortar on mitigating heat transfer and regulating thermal fluctuations within the structure. Figure 22b shows the effects of incorporating phase-change material into concrete roof in both Case 4, featuring a 3 cm PCM panel, and Case 7, featuring a 4 cm PCM panel. When comparing the results to those of Case 1, which depicts a scenario with solely concrete roof, a reduction in temperature of 3% was observed. These results highlight the importance of integrating PCM into building materials, even in small amounts, to improve thermal performance and ensure more reliable indoor comfort. As depicted in Figure 22c, replacing a 5 cm thick concrete layer with thermally reinforced

mortar resulted in a comparable temperature reduction as installing a 4 cm thick PCM panel on the concrete roof. Specifically, both Cases 3 and 7 show a 3% reduction in maximum temperature compared to Case 1. Nevertheless, these two cases present different time periods, a factor influenced by the thermal properties of phase-change materials. Moreover, Figure 22d,e show the combined effects of incorporating phase-change materials along with thermal insulation. In fact, the integration of a PCM panel between a concrete layer and a mortar layer resulted in a temperature drop that reached 43.3 °C in Case 5 and 43.2 °C in Case 8. A further improvement in thermal behavior was observed by installing the PCM panel embedded between a 5 cm thick layer of concrete and a 5 cm thick layer of textile-reinforced mortar. This integration resulted in significantly lower fluctuations in air temperature and showed a notable maximum reduction of about 4% and 5% for Case 6 and Case 9, respectively, compared to the baseline scenario. These results emphasize the collaborative effect of incorporating thermal insulation and phase-change materials into the roof structure. This synergy significantly reduces temperature fluctuations, increasing energy efficiency and therefore reducing the reliance on mechanical heating and cooling systems within buildings.

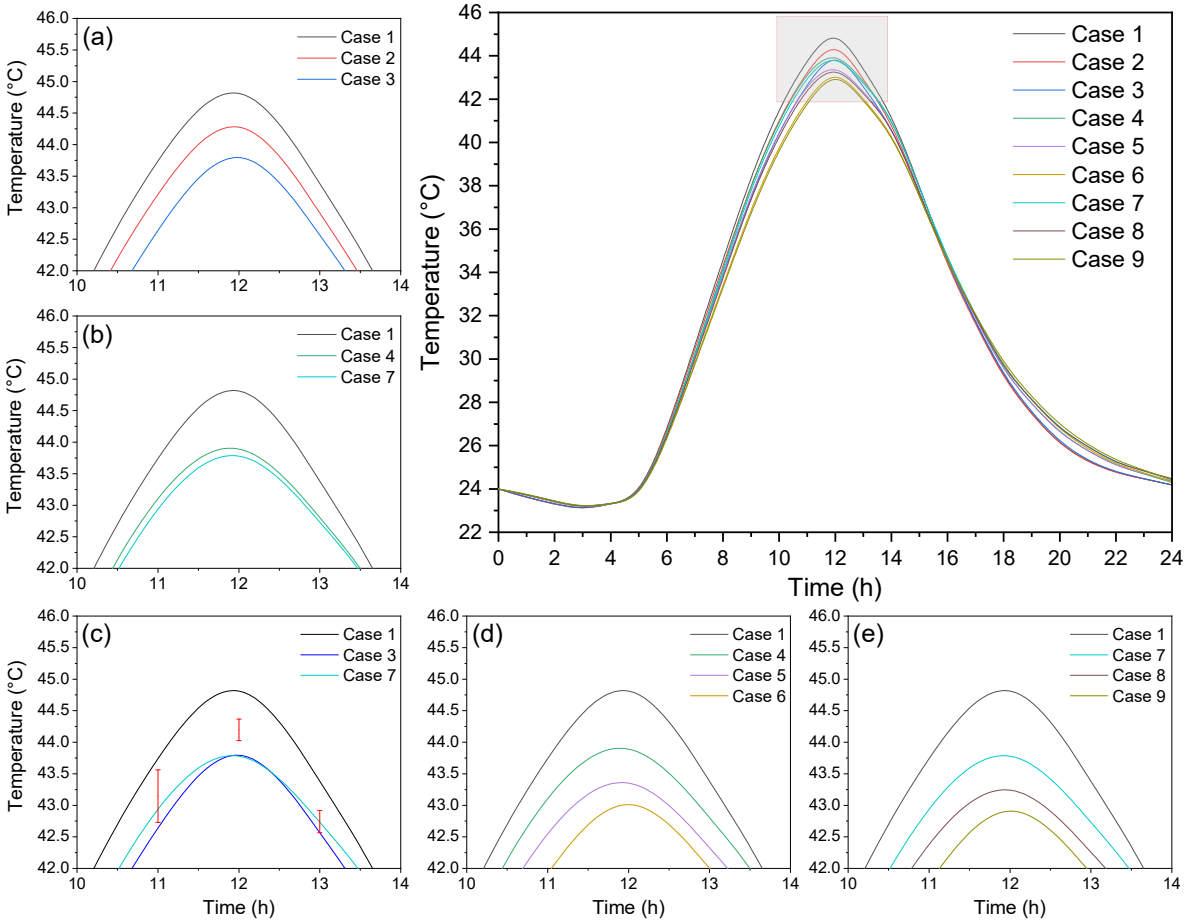
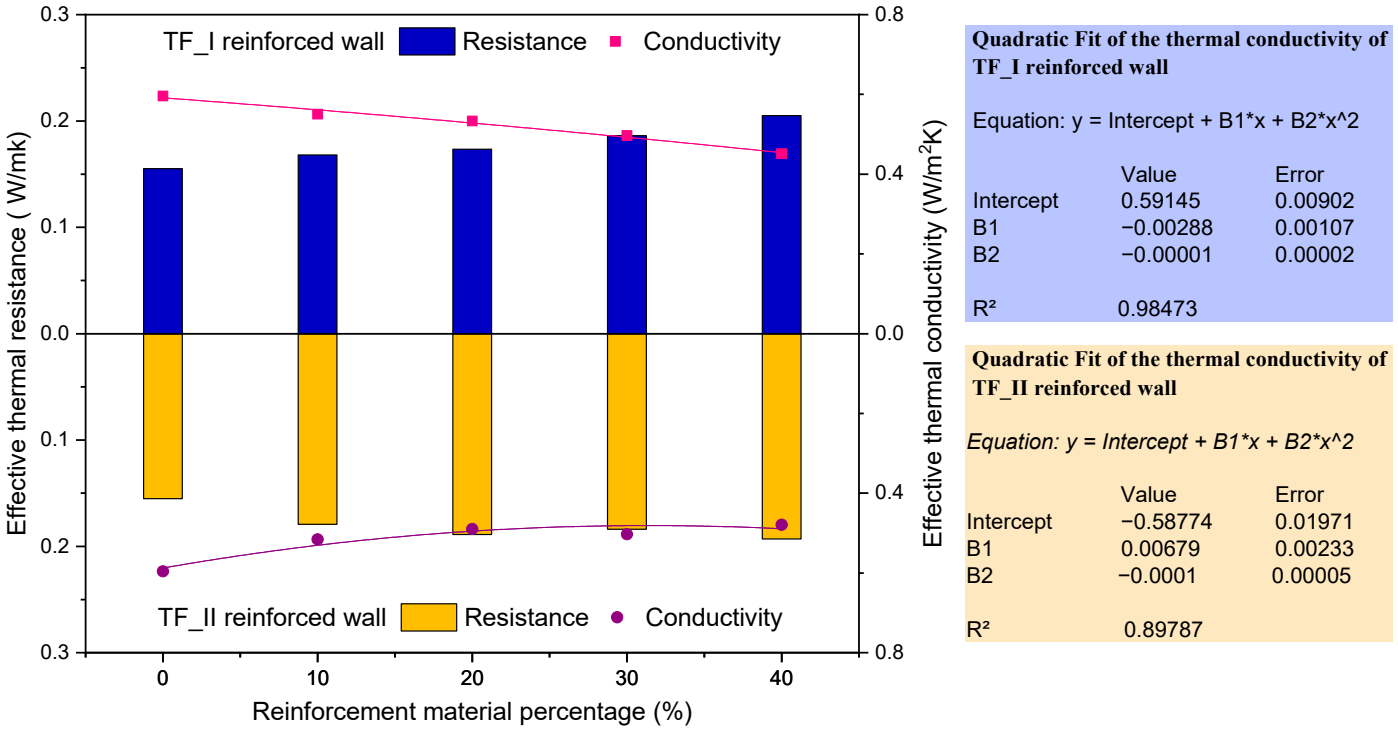


Figure 22. Comparison of air-temperature changes in all cases studied: (**a**) in Cases 1, 2 and 3, (**b**) in Cases 1, 4 and 7, (**c**) in Cases 1, 3 and 7, (**d**) in Cases 1, 4, 5 and 6, (**e**) in Cases 1, 7, 8 and 9.

6.3. Evaluation of the Effect of Adding Textile-Reinforced Mortar to the Structure of Roof and Walls

Following the examination of the effect of insulating the roof structure, this section focuses on investigating the influence of incorporating textile-reinforced mortar into the walls adjoining the roof structure. First, the changes in the effective thermal conductivity and resistance of the wall were investigated subsequent to applying textile-enhanced

mortar on both sides. Figure 23 shows the change in the effective thermal resistance and the effective thermal conductivity of the walls with increasing proportions of the two types of textile fibers in the mortar. It is clear that in both cases, effective thermal resistance increases and effective thermal conductivity decreases with increasing fiber content. As expected, TF_I mortar consistently outperforms TF_II mortar, providing a higher effective thermal resistance for a given fiber content. This is likely due to the different properties of the two fibers. TF_I is a denser fiber with a higher specific heat capacity, which makes it more effective at trapping heat and preventing it from transferring through the mortar. The results of this figure suggest that TF_I is the preferred textile fiber for use in textile fiber-reinforced mortars applications where high thermal performance is required. This is supported by the fact that TF_I was selected for use in the subsequent numerical analysis. In brief, a wall coated on both sides with a mortar reinforced with 40% TF_I fibers exhibits a thermal resistance of 0.21 W/mK and a thermal conductivity of 0.45 W/mK, showing improvements of 29% and 22%, respectively, compared to a wall coated with regular mortar.



Quadratic Fit of the thermal conductivity of TF_I reinforced wall

Equation: y = Intercept + B1*x + B2*x^2

	Value	Error
Intercept	0.59145	0.00902
B1	−0.00288	0.00107
B2	−0.00001	0.00002
R^2	0.98473	

Quadratic Fit of the thermal conductivity of TF_II reinforced wall

*Equation: y = Intercept + B1*x + B2*x^2*

	Value	Error
Intercept	−0.58774	0.01971
B1	0.00679	0.00233
B2	−0.0001	0.00005
R^2	0.89787	

Figure 23. Variation in effective thermal resistance and effective thermal conductivity with increasing percentages of two types of textile fibers.

Furthermore, four additional scenarios were studied in which the cabin consisted of brick walls coated on both sides with 40% TF_I mortar and each with a different roof structure. In Case 10, the roof is made entirely of concrete. Case 11 represents a roof consisting of a concrete layer on which a layer of TF_I reinforced mortar is applied. Case 12 involves a 4 cm thick PCM panel that is integrated directly into a concrete roof. In the last scenario (Case 13), the cabin roof contains a PCM panel sandwiched between a concrete layer and a layer of TF_I reinforced mortar. Figures 20 and 24 show the synergetic effect of insulating the roof and the walls with the reinforced textile mortar. Figure 20, which shows the temperature distribution of the cabin in a plane perpendicular to the south side, reveals that the integration of thermally reinforced mortar in the walls adjacent to the roof structure effectively reduces heat transfer, resulting in a substantial decrease in the overall temperature distribution within the cabin. Figure 24 offers a detailed overview of the spatial temperature change observed among the studied cases at four different time

periods throughout the day: 10 a.m., 12 p.m., 2 p.m., and 4 p.m. This figure provides unique insights into how changing coating materials along the roof configuration affect temperature propagation within the walls and indoor air.

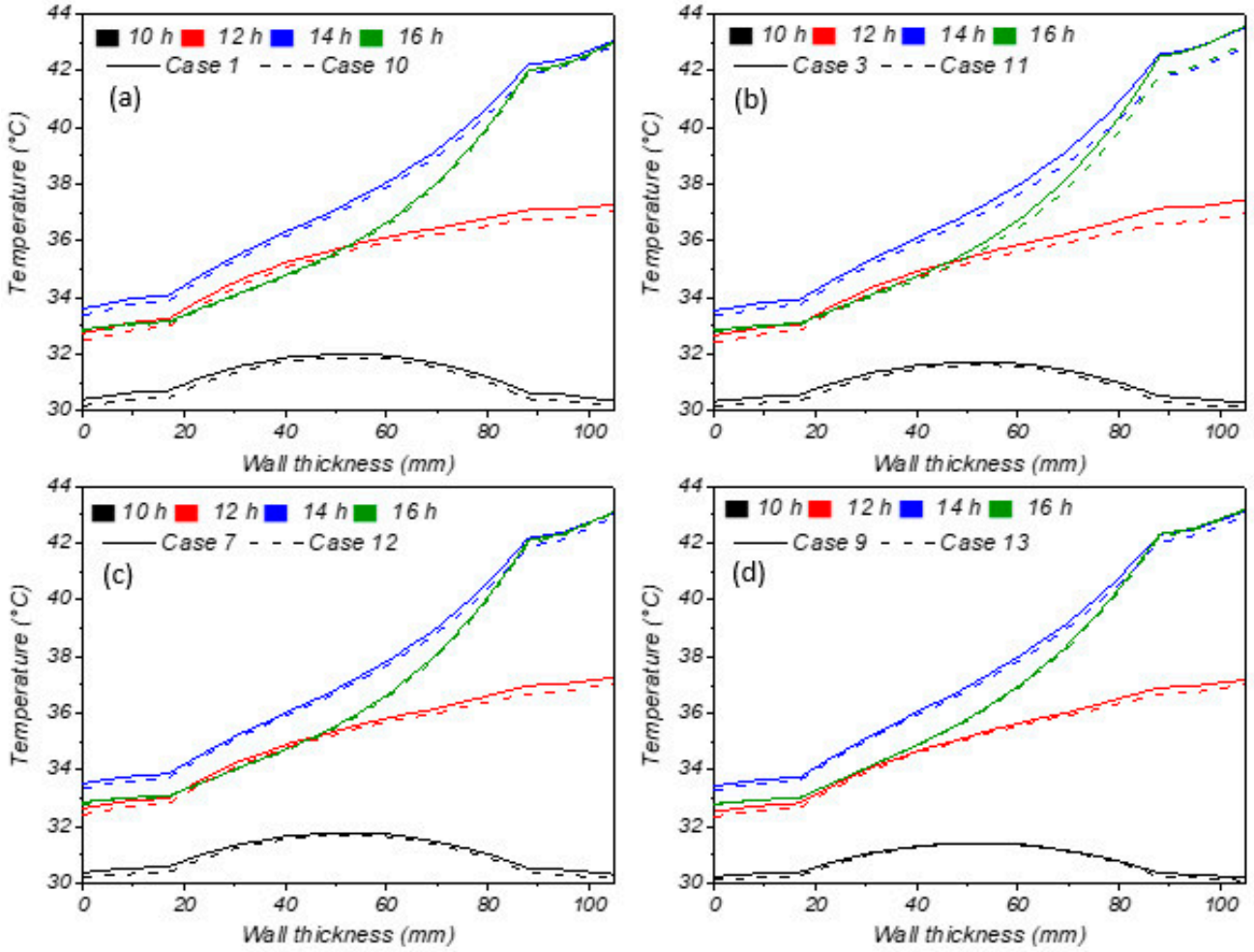


Figure 24. Spatial temperature change observed among the studied cases: (**a**) Cases 1 and 10; (**b**) Cases 3 and 11; (**c**) Cases 7 and 12; and (**d**) Cases 9 and 13, at four different time periods throughout the day.

In Figure 24a, the temperature variation across the thickness of the cabin is visualized for both Case 1 and Case 10. In both scenarios, the cabin roofs are predominantly made of concrete, but the walls are covered with different coating materials. Similarly, Figure 24b–d show the comparison of temperature change within the cabin, each time maintaining the same roof configuration but varying the wall composition. It is noteworthy that in Cases 10, 11, 12 and 13, where the wall is coated with thermally enhanced mortar, the rate of temperature propagation is slower than in the cabin with walls coated with conventional mortar. This is attributed to the fact that a wall coated with enhanced composite displays a reduced effective thermal conductivity compared to that covered by plain mortar, thereby decelerating the heat transfer process. Interestingly, the use of textile mortar as a coating material leads to favorable results in terms of attenuating temperature spread. This suggests that a balanced application of textile-enhanced composite on the entire wall surface and roof structure can effectively regulate temperature fluctuations and improve thermal efficiency.

7. Conclusions

The incorporation of recycled materials into building elements is a growing trend, driven by both ecological and technical considerations. Waste textile fibers constitute a particularly promising material for this purpose, because they make it possible to produce cement-based mortars with improved thermal properties and acceptable mechanical strength. This study investigated the potential of two types of textile fiber-reinforced mortars (TF_I and TF_II) as cladding mortars, used to cover the exterior of buildings and protect them from the elements.

Mechanical characterization tests carried out on TF_I and TF_II also indicated improved flexural strength, while compressive strength slightly decreased while meeting the requirements of the coating mortars. This suggests that textile fiber-reinforced mortars provide a viable alternative to traditional cladding mortars, with the added benefit of environmental sustainability.

A thermal analysis is carried out by the analyzer of thermal properties to determine the thermal conductivity. An analytical analysis is carried out to validate the experimentally measured thermal conductivities of the mortars reinforced with the two types of textile fibers and the values predicted by the analytical models. Then, we proceed to the development of a COMSOL numerical model, which allows us to derive the diffusivity and heat-capacity values. for the various samples. The results showed that TF_I with 40% sand replacement exhibited significant reductions in thermal conductivity, thermal diffusivity, and volumetric heat capacity, by approximately 40%, 21%, and 23%, respectively, compared with ordinary cement mortar. These improvements in thermal performance can lead to significant energy savings in buildings, particularly in hot climates.

To study in more detail the potential of TF_I fibers in building applications, a numerical study was carried out to evaluate their impact on the thermal behavior of a cabin. The study explored the potential of combining TF_I with phase-change materials (PCMs) to further improve the thermal performance of buildings. PCMs are materials capable of absorbing and releasing heat at a specific temperature, the temperature fluctuations in the cabin are determined under different conditions (from Case 1 to Case 9). The results of a numerical study showed that the combined use of TF_I and PCM on the roof of a building can reduce the maximum indoor temperature by up to 5% in summer conditions. This suggests that the combination of TF_I and PCM constitutes a promising strategy to improve the energy efficiency of buildings and reduce their dependence on air conditioning. Finally, four other cases are simulated by adding composite in the wall. The cabin walls were covered on both sides with TF_I-reinforced mortar. The results showed that covering the wall with a 20 mm layer of TF_I on both sides improved the overall thermal performance by approximately 10%. This demonstrates that TF_I can be used to effectively reduce heat transfer through building walls, thereby leading to more comfortable and energy-efficient buildings.

Overall, the results of this study suggest that textile fiber-reinforced mortars are a promising sustainable building material that can improve the thermal performance and energy efficiency of buildings. Further research is needed to optimize the formulations and applications of TF_I, but the results of this study provide a solid basis for the development of this new class of construction materials.

The study findings offer a foundation for contextualizing the potential of textile fiber-reinforced mortars (TF_I and TF_II) relative to industry benchmarks and standards in terms of both waste reduction and energy efficiency. The use of used textile fibers directly addresses the global challenge of textile waste management, which aligns with sustainability objectives outlined in frameworks such as the European Green Deal or the United Nations Sustainable Development Goals (e.g., Goal 12: responsible consumption and production). By incorporating a 40% replacement of sand with textile fibers in TF_I, the material demon-

strates significant resource conservation compared to traditional cement mortars. Industry benchmarks such as ISO 14001 [141] for environmental management could be used to quantify reductions in raw material consumption and waste generation. The thermal performance improvements achieved with TF_I, including the 40% reduction in thermal conductivity, directly contribute to energy savings in buildings. Compared to traditional building materials, this reduction is significant and could be contextualized using standards such as ASHRAE 90.1 [142] (energy standard for buildings) or ISO 13790:2008 [143], which guide the design of energy-efficient buildings. The 5% reduction in maximum indoor temperatures in summer achieved with TF_I and the integration of PCM highlights its potential to reduce cooling energy requirements, a critical factor in hot-climate regions. To fully integrate textile fiber-reinforced mortars into mainstream construction practices, it will be necessary to establish industry standards for their use, including performance, durability, and environmental impact. Future work could include comparing these materials to existing industry standards such as ISO 14001 [141] for environmental sustainability to highlight their benefits and broaden their application.

The lifecycle of textile-reinforced mortars shows significant environmental impacts during the production of textile fibers and the cement matrix due to high energy use and emissions. However, TRMs' excellent durability reduces the need for frequent repairs, lowering resource consumption and waste over time. Recycling remains a major challenge, as separating textiles from the cement matrix is difficult, often resulting in landfilling. Advancements in recycling technologies and the use of more sustainable materials could improve end-of-life solutions, reducing embodied carbon and maintenance costs while enhancing their overall environmental performance.

Author Contributions: Conceptualization, R.A. and S.B.; Methodology, R.A., E.B. and S.B.; Software, R.A.; Validation, R.A., S.S. and S.B.; Formal analysis, R.A., S.S., M.L. (Mohamed Lachheb) and S.B.; Investigation, R.A. and E.B.; Resources, Z.Y., L.F.C. and M.L. (Mariem Lazaar); Data curation, R.A. and E.B.; Writing—original draft, R.A., S.S. and S.B.; Writing—review & editing, R.A., S.B., Z.Y. and L.F.C.; Visualization, R.A., M.L. (Mohamed Lachheb) and S.B.; Supervision, L.F.C. and M.L. (Mariem Lazaar); Project administration, L.F.C.; Funding acquisition, L.F.C. All authors have read and agreed to the published version of the manuscript.

Funding: This study was supported by the Thermal Processes Laboratory of the Research and Technology Center of Energy (CRTEn) and the University of Tunis El Manar in Tunisia. This work was partially funded by the Ministerio de Ciencia e Innovación—Agencia Estatal de Investigación (AEI) (PID2021-123511OB-C31—MCIN/AEI/10.13039/501100011033/FEDER, UE and RED2022-134219-T). This publication is based upon work from COST Action CircularB, supported by COST (European Cooperation in Science and Technology). This work is partially supported by ICREA under the ICREA Academia programme.

Data Availability Statement: The original contributions presented in this study are included in the article. Further inquiries can be directed to the corresponding author.

Acknowledgments: The authors from GREiA Research Group would like to thank the Catalan Government for the quality accreditation given to their research group GREiA (2021 SGR 01615). GREiA is a certified agent TECNIO in the category of technology developers from the Government of Catalonia. This work is partially supported by ICREA under the ICREA Academia programme. This paper is part of the RYC2023-044196-I, funded by MCIU/AEI/10.13039/501100011033 and FSE+.

Conflicts of Interest: The authors declare no conflicts of interest.

References

1. Ukhurebor, K.E.; Ngonso, B.F.; Egielewa, P.E.; Cirella, G.T.; Akinsehinde, B.O.; Balogune, V.A. Petroleum Spills and the Communicative Response from Petroleum Agencies and Companies: Impact Assessment from the Niger Delta Region of Nigeria. *Extr. Ind. Soc.* **2023**, *15*, 101331. [CrossRef]
2. Furszyfer Del Rio, D.D.; Sovacool, B.K.; Griffiths, S.; Bazilian, M.; Kim, J.; Foley, A.M.; Rooney, D. Decarbonizing the Pulp and Paper Industry: A Critical and Systematic Review of Sociotechnical Developments and Policy Options. *Renew. Sustain. Energy Rev.* **2022**, *167*, 112706. [CrossRef]
3. Reichle, D.E. Carbon, Climate Change, and Public Policy. In *The Global Carbon Cycle and Climate Change*; Elsevier: Amsterdam, The Netherlands, 2023; pp. 503–570, ISBN 9780443187759. [CrossRef]
4. Gao, Q.; Li, X.G.; Jiang, S.Q.; Lyu, X.J.; Gao, X.; Zhu, X.N.; Zhang, Y.Q. Review on Zero Waste Strategy for Urban Construction and Demolition Waste: Full Component Resource Utilization Approach for Sustainable and Low-Carbon. *Constr. Build. Mater.* **2023**, *395*, 132354. [CrossRef]
5. Gholami Rostam, M.; Abbasi, A. Integrating Construction and Demolition Waste Impact Categories into Building Energy Optimization through a Conceptual Sustainability-Oriented Model. *J. Clean. Prod.* **2022**, *378*, 134543. [CrossRef]
6. Bergonzoni, M.; Melloni, R.; Botti, L. Analysis of Sustainable Concrete Obtained from the By-Products of an Industrial Process and Recycled Aggregates from Construction and Demolition Waste. *Procedia Comput. Sci.* **2022**, *217*, 41–51. [CrossRef]
7. Oberle, B.; Bringezu, S.; Hatfield-Dodds, S.; Hellweg, S.; Schandl, H.; Clement, J.; Cabernard, L.; Che, N.; Chen, D.; Droz-Georget, H.; et al. *Global Resources Outlook 2019: Natural Resources for the Future We Want*; United Nations Environment Programme: Nairobi, Kenya, 2019; ISBN 9789280737417.
8. International Energy Agency (IEA). Empowering Cities for a Net Zero Future: Unlocking Resilient, Smart. In *Sustainable Urban Energy Systems*; International Energy Agency (IEA): Paris, France, 2021.
9. *REGULATION (EU) No 305/2011*; Laying Down Harmonised Conditions for the Marketing of Construction Products and Repealing Council Directive 89/106/EEC. Official Journal of the European Union: Brussels, Belgium, 2011.
10. U.S. Green Building Council (USGBC). Rating System Overview: Leadership in Energy and Environmental Design. Available online: https://www.usgbc.org/leed (accessed on 15 January 2025).
11. International Code Council (ICC); International Building Code (IBC). Available online: https://www.iccsafe.org/ (accessed on 15 January 2025).
12. Hossain, M.U.; Ng, S.T.; Antwi-Afari, P.; Amor, B. Circular Economy and the Construction Industry: Existing Trends, Challenges and Prospective Framework for Sustainable Construction. *Renew. Sustain. Energy Rev.* **2020**, *130*, 109948. [CrossRef]
13. Dsilva, J.; Zarmukhambetova, S.; Locke, J. Assessment of Building Materials in the Construction Sector: A Case Study Using Life Cycle Assessment Approach to Achieve the Circular Economy. *Heliyon* **2023**, *9*, e20404. [CrossRef] [PubMed]
14. Geissdoerfer, M.; Savaget, P.; Bocken, N.M.P.; Hultink, E.J. The Circular Economy—A New Sustainability Paradigm? *J. Clean. Prod.* **2017**, *143*, 757–768. [CrossRef]
15. Bukar, U.A.; Sayeed, M.S.; Razak, S.F.A.; Yogarayan, S.; Amodu, O.A.; Mahmood, R.A.R. A Method for Analyzing Text Using VOSviewer. *MethodsX* **2023**, *11*, 102339. [CrossRef]
16. International Energy Agency (IEA). *Net Zero by 2050: A Roadmap for the Global Energy Sector*; International Energy Agency (IEA): Paris, France, 2021.
17. Baddadi, S.; Bouadila, S.; Guizani, A. Beneficial Use of Two Packed Beds of Latent Storage Energy for the Heating of a Hydroponic Greenhouse. *Energy Procedia* **2019**, *162*, 156–163. [CrossRef]
18. Bouadila, S.; Baddadi, S.; Skouri, S.; Ayed, R. Assessing Heating and Cooling Needs of Hydroponic Sheltered System in Mediterranean Climate: A Case Study Sustainable Fodder Production. *Energy* **2022**, *261*, 125274. [CrossRef]
19. González-Torres, M.; Pérez-Lombard, L.; Coronel, J.F.; Maestre, I.R.; Yan, D. A Review on Buildings Energy Information: Trends, End-Uses, Fuels and Drivers. *Energy Rep.* **2022**, *8*, 626–637. [CrossRef]
20. Paraschiv, S.; Paraschiv, L.S.; Serban, A. Increasing the Energy Efficiency of a Building by Thermal Insulation to Reduce the Thermal Load of the Micro-Combined Cooling, Heating and Power System. *Energy Rep.* **2021**, *7*, 286–298. [CrossRef]
21. Aste, N.; Leonforte, F.; Manfren, M.; Mazzon, M. Thermal Inertia and Energy Efficiency—Parametric Simulation Assessment on a Calibrated Case Study. *Appl. Energy* **2015**, *145*, 111–123. [CrossRef]
22. Zach, J.; Novak, V.; Peterkova, J.; Bubenik, J.; Kosir, M.; Bozicek, D.; Krejza, Z. The Use of Advanced Environmentally Friendly Systems in the Insulation and Reconstruction of Buildings. *Buildings* **2023**, *13*, 404. [CrossRef]
23. Armenia, S.; Arquitt, S.; Pedercini, M.; Pompei, A. Anticipating Human Resilience and Vulnerability on the Path to 2030: What Can We Learn from COVID-19? *Futures* **2022**, *139*, 102936. [CrossRef]
24. Habicher, D.; Windegger, F.; von der Gracht, H.A.; Pechlaner, H. Beyond the COVID-19 Crisis: A Research Note on Post-Pandemic Scenarios for South Tyrol 2030+. *Technol. Forecast. Soc. Change* **2022**, *180*, 121749. [CrossRef] [PubMed]

25. Bouadil, S.; Skouri, S.; Kooli, S.; Lazaar, M.; Farhat, A. Solar Energy Storage Application in Tunisian Greenhouse by Means of Phase Change Materials. In Proceedings of the 2014 International Conference on Composite Materials & Renewable Energy Applications (ICCMREA), Sousse, Tunisia, 22–24 January 2014; pp. 1–4. [CrossRef]
26. Cabeza, L.F.; Chàfer, M. Technological Options and Strategies towards Zero Energy Buildings Contributing to Climate Change Mitigation: A Systematic Review. *Energy Build.* **2020**, *219*, 110009. [CrossRef]
27. Nagy, Z.; Yong, F.Y.; Frei, M.; Schlueter, A. Occupant Centered Lighting Control for Comfort and Energy Efficient Building Operation. *Energy Build.* **2015**, *94*, 100–108. [CrossRef]
28. Yudelson, J. *The Green-Building Revolution*; Island Press: Washington, DC, USA, 2008.
29. Darko, A.; Chan, A.P.C. Critical Analysis of Green Building Research Trend in Construction Journals. *Habitat Int.* **2016**, *57*, 53–63. [CrossRef]
30. Worden, K.; Hazer, M.; Pyke, C.; Trowbridge, M. Using LEED Green Rating Systems to Promote Population Health. *Build. Environ.* **2020**, *172*, 106550. [CrossRef]
31. Moh, Y.C.; Abd Manaf, L. Solid Waste Management Transformation and Future Challenges of Source Separation and Recycling Practice in Malaysia. *Resour. Conserv. Recycl.* **2017**, *116*, 1–14. [CrossRef]
32. Van Den Heede, P.; De Belie, N. Environmental Impact and Life Cycle Assessment (LCA) of Traditional and 'Green' Concretes: Literature Review and Theoretical Calculations. *Cem. Concr. Compos.* **2012**, *34*, 431–442. [CrossRef]
33. Nuñez-Cacho, P.; Górecki, J.; Molina-Moreno, V.; Corpas-Iglesias, F.A. What Gets Measured, Gets Done: Development of a Circular Economy Measurement Scale for Building Industry. *Sustainability* **2018**, *10*, 2340. [CrossRef]
34. Cintura, E.; Nunes, L.; Esteves, B.; Faria, P. Agro-Industrial Wastes as Building Insulation Materials: A Review and Challenges for Euro-Mediterranean Countries. *Ind. Crops Prod.* **2021**, *171*, 113833. [CrossRef]
35. Francioso, V.; Moro, C.; Velay-Lizancos, M. Effect of Recycled Concrete Aggregate (RCA) on Mortar's Thermal Conductivity Susceptibility to Variations of Moisture Content and Ambient Temperature. *J. Build. Eng.* **2021**, *43*, 103208. [CrossRef]
36. Letelier, V.; Bustamante, M.; Muñoz, P.; Rivas, S.; Ortega, J.M. Evaluation of Mortars with Combined Use of Fine Recycled Aggregates and Waste Crumb Rubber. *J. Build. Eng.* **2021**, *43*, 103226. [CrossRef]
37. Benyamina, S.; Abadou, Y.; Ghrieb, A. Thermal Properties of Dune Sand Based-Rubber Mortar Composites. *Mater. Today Proc.* **2021**, *56*, 2199–2203. [CrossRef]
38. Selvaranjan, K.; Gamage, J.C.P.H.; De Silva, G.I.P.; Navaratnam, S. Development of Sustainable Mortar Using Waste Rice Husk Ash from Rice Mill Plant: Physical and Thermal Properties. *J. Build. Eng.* **2021**, *43*, 102614. [CrossRef]
39. Badache, A.; Benosman, A.S.; Senhadji, Y.; Mouli, M. Thermo-Physical and Mechanical Characteristics of Sand-Based Lightweight Composite Mortars with Recycled High-Density Polyethylene (HDPE). *Constr. Build. Mater.* **2018**, *163*, 40–52. [CrossRef]
40. Borinaga- Treviño, R.; Cuadrado, J.; Canales, J.; Rojí, E. Lime Mud Waste from the Paper Industry as a Partial Replacement of Cement in Mortars Used on Radiant Floor Heating Systems. *J. Build. Eng.* **2021**, *41*, 102408. [CrossRef]
41. Batool, F.; Rafi, M.M.; Bindiganavile, V. Microstructure and Thermal Conductivity of Cement-Based Foam: A Review. *J. Build. Eng.* **2018**, *20*, 696–704. [CrossRef]
42. Salem, T.; Fois, M.; Omikrine-Metalssi, O.; Manuel, R.; Fen-Chong, T. Thermal and Mechanical Performances of Cement-Based Mortars Reinforced with Vegetable Synthetic Sponge Wastes and Silica Fume. *Constr. Build. Mater.* **2020**, *264*, 120213. [CrossRef]
43. Taoukil, D.; El meski, Y.; lhassane Lahlaouti, M.; Djedjig, R.; El bouardi, A. Effect of the Use of Diatomite as Partial Replacement of Sand on Thermal and Mechanical Properties of Mortars. *J. Build. Eng.* **2021**, *42*, 103038. [CrossRef]
44. Torres-Carrasco, M.; Enríquez, E.; Terrón-Menoyo, L.; Cabrera, M.J.; Muñoz, D.; Fernández, J.F. Improvement of Thermal Efficiency in Cement Mortars by Using Synthetic Feldspars. *Constr. Build. Mater.* **2021**, *269*, 121279. [CrossRef]
45. Srikanth, G.; Fernando, A.; Selvaranjan, K.; Gamage, J.C.P.H.; Ekanayake, L. Development of a Plastering Mortar Using Waste Bagasse and Rice Husk Ashes with Sound Mechanical and Thermal Properties. *Case Stud. Constr. Mater.* **2022**, *16*, e00956. [CrossRef]
46. Senhadji, Y.; Siad, H.; Escadeillas, G.; Benosman, A.S.; Chihaoui, R.; Mouli, M.; Lachemi, M. Physical, Mechanical and Thermal Properties of Lightweight Composite Mortars Containing Recycled Polyvinyl Chloride. *Constr. Build. Mater.* **2019**, *195*, 198–207. [CrossRef]
47. Bostanci, L. A Comparative Study of Petroleum Coke and Silica Aerogel Inclusion on Mechanical, Pore Structure, Thermal Conductivity and Microstructure Properties of Hybrid Mortars. *J. Build. Eng.* **2020**, *31*, 101478. [CrossRef]
48. Liu, Y.; Cao, Z.; Wang, Y.; Wang, D.; Liu, J. Experimental Study of Hygro-Thermal Characteristics of Novel Cement-Cork Mortars. *Constr. Build. Mater.* **2021**, *271*, 121901. [CrossRef]
49. Kim, J.; Yi, C.; Zi, G. Waste Glass Sludge as a Partial Cement Replacement in Mortar. *Constr. Build. Mater.* **2015**, *75*, 242–246. [CrossRef]
50. Bergmann Becker, P.F.; Effting, C.; Schackow, A. Lightweight Thermal Insulating Coating Mortars with Aerogel, EPS, and Vermiculite for Energy Conservation in Buildings. *Cem. Concr. Compos.* **2022**, *125*, 104283. [CrossRef]

51. Mo, K.H.; Lee, H.J.; Liu, M.Y.J.; Ling, T.C. Incorporation of Expanded Vermiculite Lightweight Aggregate in Cement Mortar. *Constr. Build. Mater.* **2018**, *179*, 302–306. [CrossRef]
52. Koksal, F.; Nazlı, T.; Benli, A.; Gencel, O.; Kaplan, G. The Effects of Cement Type and Expanded Vermiculite Powder on the Thermo-Mechanical Characteristics and Durability of Lightweight Mortars at High Temperature and RSM Modelling. *Case Stud. Constr. Mater.* **2021**, *15*, e00709. [CrossRef]
53. Fayed, S.; Madenci, E.; Özkiliç, Y.O.; Tawfik, T.A. Effect of Block Size on Bearing Strength of Steel Fiber-Reinforced Recycled Aggregate Concrete. *Arab. J. Sci. Eng.* **2024**, *49*, 5287–5303. [CrossRef]
54. Fayed, S.; Madenci, E.; Onuralp Özkiliç, Y.; Mansour, W. Improving Bond Performance of Ribbed Steel Bars Embedded in Recycled Aggregate Concrete Using Steel Mesh Fabric Confinement. *Constr. Build. Mater.* **2023**, *369*, 130452. [CrossRef]
55. Ecemiş, A.S.; Madenci, E.; Karalar, M.; Fayed, S.; Althaqafi, E.; Özkılıç, Y.O. Shear Performance of Reinforced Concrete Beams with Rubber as Form of Fiber from Waste Tire. *Steel Compos. Struct.* **2024**, *51*, 337–349. [CrossRef]
56. Zhu, Q.; Chen, J.; He, Y.; Sun, X. Bond Stress Distribution and Bond–Slip Model of Deformed Steel Bars in Iron Tailing Sand Recycled Aggregate Concrete. *Buildings* **2023**, *13*, 1176. [CrossRef]
57. Piscicelli, L.; Cooper, T.; Fisher, T. The Role of Values in Collaborative Consumption: Insights from a Product-Service System for Lending and Borrowing in the UK. *J. Clean. Prod.* **2015**, *97*, 21–29. [CrossRef]
58. Franceschini, S.; Faria, L.G.D.; Jurowetzki, R. Unveiling Scientific Communities about Sustainability and Innovation. A Bibliometric Journey around Sustainable Terms. *J. Clean. Prod.* **2016**, *127*, 72–83. [CrossRef]
59. López Ruiz, L.A.; Roca Ramón, X.; Gassó Domingo, S. The Circular Economy in the Construction and Demolition Waste Sector—A Review and an Integrative Model Approach. *J. Clean. Prod.* **2020**, *248*, 119238. [CrossRef]
60. Mhatre, P.; Gedam, V.; Unnikrishnan, S.; Verma, S. Circular Economy in Built Environment—Literature Review and Theory Development. *J. Build. Eng.* **2021**, *35*, 101995. [CrossRef]
61. Norouzi, M.; Chàfer, M.; Cabeza, L.F.; Jiménez, L.; Boer, D. Circular Economy in the Building and Construction Sector: A Scientific Evolution Analysis. *J. Build. Eng.* **2021**, *44*, 102704. [CrossRef]
62. Paiho, S.; Wessberg, N.; Pippuri-Mäkeläinen, J.; Mäki, E.; Sokka, L.; Parviainen, T.; Nikinmaa, M.; Siikavirta, H.; Paavola, M.; Antikainen, M.; et al. Creating a Circular City—An Analysis of Potential Transportation, Energy and Food Solutions in a Case District. *Sustain. Cities Soc.* **2021**, *64*, 102529. [CrossRef]
63. Corinaldesi, V.; Moriconi, G. Influence of Mineral Additions on the Performance of 100% Recycled Aggregate Concrete. *Constr. Build. Mater.* **2009**, *23*, 2869–2876. [CrossRef]
64. Det Udomsap, A.; Hallinger, P. A Bibliometric Review of Research on Sustainable Construction, 1994–2018. *J. Clean. Prod.* **2020**, *254*, 120073. [CrossRef]
65. Benachio, G.L.F.; Freitas, M.d.C.D.; Tavares, S.F. Circular Economy in the Construction Industry: A Systematic Literature Review. *J. Clean. Prod.* **2020**, *260*, 121046. [CrossRef]
66. Ayed, R.; Baddadi, S.; Bouadila, S.; Skouri, S.; Lazaar, M. Architectural Development of the Buildings' Envelope to Improve Energy Efficiency. In *Advances in Science, Technology and Innovation*; Springer International Publishing: Cham, Switzerland, 2022; pp. 459–461, ISBN 9783031008085.
67. Zhao, J.; Li, S. Life Cycle Cost Assessment and Multi-Criteria Decision Analysis of Environment-Friendly Building Insulation Materials—A Review. *Energy Build.* **2022**, *254*, 111582. [CrossRef]
68. Vera, R.E.; Suarez, A.; Zambrano, F.; Marquez, R.; Bedard, J.; Vivas, K.A.; Pifano, A.; Farrell, M.; Ankeny, M.; Jameel, H.; et al. Upcycling Cotton Textile Waste into Bio-Based Building Blocks through an Environmentally Friendly and High-Yield Conversion Process. *Resour. Conserv. Recycl.* **2023**, *189*, 106715. [CrossRef]
69. Ayed, R.; Bouadila, S.; Skouri, S.; Boquera, L.; Cabeza, L.F.; Lazaar, M. Recycling Textile Waste to Enhance Building Thermal Insulation and Reduce Carbon Emissions: Experimentation and Model-Based Dynamic Assessment. *Buildings* **2023**, *13*, 535. [CrossRef]
70. Ayed, R.; Dellagi, A.; Skouri, S.; Baddadi, S.; Bouadila, S. Sustainable Insulation Solutions for Hydroponic Greenhouses: The Effects of Textile Waste Reinforcement on Thermal Microclimate. *J. Build. Eng.* **2023**, *73*, 106710. [CrossRef]
71. Azzouzi, D.; Rabahi, W.; Seddiri, F.; Hemis, M. Experimental Study of the Fibres Content Effect on the Heat Insulation Capacity of New Vegetable Composite Plaster-Pea Pod Fibres. *Sustain. Mater. Technol.* **2020**, *23*, e00144. [CrossRef]
72. Zhang, J.; Wang, J.; Guo, S.; Wei, B.; He, X.; Sun, J.; Shu, S. Study on Heat Transfer Characteristics of Straw Block Wall in Solar Greenhouse. *Energy Build.* **2017**, *139*, 91–100. [CrossRef]
73. Jiang, D.; Lv, S.; Cui, S.; Sun, S.; Song, X.; He, S.; Zhang, J.; An, P. Effect of Thermal Insulation Components on Physical and Mechanical Properties of Plant Fibre Composite Thermal Insulation Mortar. *J. Mater. Res. Technol.* **2020**, *9*, 12996–13013. [CrossRef]
74. Briga-Sá, A.; Nascimento, D.; Teixeira, N.; Pinto, J.; Caldeira, F.; Varum, H.; Paiva, A. Textile Waste as an Alternative Thermal Insulation Building Material Solution. *Constr. Build. Mater.* **2013**, *38*, 155–160. [CrossRef]

75. Ntimugura, F.; Vinai, R.; Harper, A.; Walker, P. Mechanical, Thermal, Hygroscopic and Acoustic Properties of Bio-Aggregates—Lime and Alkali—Activated Insulating Composite Materials: A Review of Current Status and Prospects for Miscanthus as an Innovative Resource in the South West of England. *Sustain. Mater. Technol.* **2020**, *26*, e00211. [CrossRef]
76. Sandanayake, M.; Gunasekara, C.; Law, D.; Zhang, G.; Setunge, S.; Wanijuru, D. Sustainable Criterion Selection Framework for Green Building Materials—An Optimisation Based Study of Fly-Ash Geopolymer Concrete. *Sustain. Mater. Technol.* **2020**, *25*, e00178. [CrossRef]
77. Quiñones-Bolaños, E.; Gómez-Oviedo, M.; Mouthon-Bello, J.; Sierra-Vitola, L.; Berardi, U.; Bustillo-Lecompte, C. Potential Use of Coconut Fibre Modified Mortars to Enhance Thermal Comfort in Low-Income Housing. *J. Environ. Manag.* **2021**, *277*, 111503. [CrossRef] [PubMed]
78. Balo, F.; Ulutas, A. Energy-Performance Evaluation with Revit Analysis of Mathematical-Model-Based Optimal Insulation Thickness. *Buildings* **2023**, *13*, 408. [CrossRef]
79. Majumder, A.; Canale, L.; Mastino, C.C.; Pacitto, A.; Frattolillo, A.; Dell'isola, M. Thermal Characterization of Recycled Materials for Building Insulation. *Energies* **2021**, *14*, 3564. [CrossRef]
80. Rosca, B.; Corobceanu, V. Structural Grade Concrete Containing Expanded Polystyrene Beads with Different Particle Distributions of Normal Weight Aggregate. *Mater. Today Proc.* **2020**, *42*, 548–554. [CrossRef]
81. Gencel, O.; Yavuz Bayraktar, O.; Kaplan, G.; Arslan, O.; Nodehi, M.; Benli, A.; Gholampour, A.; Ozbakkaloglu, T. Lightweight Foam Concrete Containing Expanded Perlite and Glass Sand: Physico-Mechanical, Durability, and Insulation Properties. *Constr. Build. Mater.* **2022**, *320*, 126187. [CrossRef]
82. Li, J.; Meng, X.; Gao, Y.; Mao, W.; Luo, T.; Zhang, L. Effect of the Insulation Materials Filling on the Thermal Performance of Sintered Hollow Bricks. *Case Stud. Therm. Eng.* **2018**, *11*, 62–70. [CrossRef]
83. Ayed, R.; Baddadi, S.; Dellagi, A.; Bouadila, S.; Lazaar, M. Thermal Behavior Improvement of Building Materials Using Expanded Polystyrene. In Proceedings of the 2022 13th International Renewable Energy Congress (IREC), Hammamet, Tunisia, 13–15 December 2022; IEEE: New York, NY, USA, 2022; pp. 13–16.
84. Lachheb, M.; Younsi, Z.; Youssef, N.; Bouadila, S. Enhancing Building Energy Efficiency and Thermal Performance with PCM-Integrated Brick Walls: A Comprehensive Review. *Build. Environ.* **2024**, *256*, 111476. [CrossRef]
85. Akinyemi, B.A.; Dai, C. Development of Banana Fibers and Wood Bottom Ash Modified Cement Mortars. *Constr. Build. Mater.* **2020**, *241*, 118041. [CrossRef]
86. Kochova, K.; Gauvin, F.; Schollbach, K.; Brouwers, H.J.H. Using Alternative Waste Coir Fibres as a Reinforcement in Cement-Fibre Composites. *Constr. Build. Mater.* **2020**, *231*, 117121. [CrossRef]
87. Cardinale, T.; Arleo, G.; Bernardo, F.; Feo, A.; De Fazio, P. Thermal and Mechanical Characterization of Panels Made by Cement Mortar and Sheep's Wool Fibres. *Energy Procedia* **2017**, *140*, 159–169. [CrossRef]
88. de Azevedo, A.R.G.; Marvila, M.T.; Tayeh, B.A.; Cecchin, D.; Pereira, A.C.; Monteiro, S.N. Technological Performance of Açaí Natural Fibre Reinforced Cement-Based Mortars. *J. Build. Eng.* **2021**, *33*, 101675. [CrossRef]
89. Rama Rao, P.; Ramakrishna, G. Experimental Investigation on Mechanical Properties of Oil Palm Empty Fruit Bunch Fiber Reinforced Cement Mortar. *Mater. Today Proc.* **2021**, *46*, 471–477. [CrossRef]
90. Benmansour, N.; Agoudjil, B.; Gherabli, A.; Kareche, A.; Boudenne, A. Thermal and Mechanical Performance of Natural Mortar Reinforced with Date Palm Fibers for Use as Insulating Materials in Building. *Energy Build.* **2014**, *81*, 98–104. [CrossRef]
91. Awoyera, P.O.; Akinrinade, A.D.; de Sousa Galdino, A.G.; Althoey, F.; Kirgiz, M.S.; Tayeh, B.A. Thermal Insulation and Mechanical Characteristics of Cement Mortar Reinforced with Mineral Wool and Rice Straw Fibers. *J. Build. Eng.* **2022**, *53*, 104568. [CrossRef]
92. Borinaga-Treviño, R.; Orbe, A.; Canales, J.; Norambuena-Contreras, J. Thermal and Mechanical Properties of Mortars Reinforced with Recycled Brass Fibres. *Constr. Build. Mater.* **2021**, *284*, 122832. [CrossRef]
93. Zhang, X.; He, W.; Zhang, Y.; Chen, C.; Wu, X. Tensile Behavior of Basalt-Fiber-Grid-Reinforced Mortar before and after Exposure to Elevated Temperature. *Buildings* **2022**, *12*, 2269. [CrossRef]
94. Lizundia, E. Organic Waste Valorisation towards Circular and Sustainable Biocomposites. *Green Chem.* **2022**, *24*, 5429–5459. [CrossRef]
95. Ayed, R.; Borri, E.; Zsembinszki, G.; Bouadila, S.; Cabeza, L.F.; Lazaar, M. *Use of Textile Fiber Waste to Improve the Thermal and Mechanical Performance of Cement-Based Mortar*; Springer Nature: Cham, Switzerland, 2024; Volume 489, ISBN 9783031577994.
96. Ayed, R.; Borri, E.; Gasa, G.; Bouadila, S.; Cabeza, L.F. An Experimental Study on the Thermo-Mechanical Properties of Cement Mortar with Textile Fibers for Building Applications. *RILEM Bookseries* **2023**, *43*, 1153–1162. [CrossRef]
97. Zhou, X.Y.; Ruan, X.; Zhang, S.; Xiong, W.; Ullah, Z. Design Optimization for Thermal Conductivity of Plain-Woven Textile Composites. *Compos. Struct.* **2021**, *255*, 112830. [CrossRef]
98. Briga-Sá, A.; Gaibor, N.; Magalhães, L.; Pinto, T.; Leitão, D. Thermal Performance Characterization of Cement-Based Lightweight Blocks Incorporating Textile Waste. *Constr. Build. Mater.* **2022**, *321*, 126330. [CrossRef]
99. Koutas, L.N.; Papakonstantinou, C.G. Flexural Strengthening of RC Beams with Textile-Reinforced Mortar Composites Focusing on the Influence of the Mortar Type. *Eng. Struct.* **2021**, *246*, 113060. [CrossRef]

100. Zhang, H.Y.; Liu, H.Y.; Kodur, V.; Li, M.Y.; Zhou, Y. Flexural Behavior of Concrete Slabs Strengthened with Textile Reinforced Geopolymer Mortar. *Compos. Struct.* **2022**, *284*, 115220. [CrossRef]
101. Adheem, A.H.; Kadhim, M.M.A.; Jawdhari, A.; Fam, A. Confinement Model for Concrete Wrapped with Fiber Reinforced Cementitious Mortar. *Constr. Build. Mater.* **2021**, *312*, 125401. [CrossRef]
102. Dinh, N.H.; Van Tran, H.; Choi, K.K. Direct Shear Behavior of Cementitious Mortar Reinforced by Carbon Fiber Textile. *Constr. Build. Mater.* **2020**, *249*, 118760. [CrossRef]
103. Brazão Farinha, C.; de Brito, J.; Veiga, R. Incorporation of High Contents of Textile, Acrylic and Glass Waste Fibres in Cement-Based Mortars. Influence on Mortars' Fresh, Mechanical and Deformability Behaviour. *Constr. Build. Mater.* **2021**, *303*, 124424. [CrossRef]
104. Shamseldein, A.; ELgabbas, F.; Elshafie, H. Tensile Behavior of Basalt Textile-Reinforced Mortar (BTRM). *Ain Shams Eng. J.* **2022**, *13*, 101488. [CrossRef]
105. Mercimek, Ö.; Ghoroubi, R.; Özdemir, A.; Anil, Ö.; Erbaş, Y. Investigation of Strengthened Low Slenderness RC Column by Using Textile Reinforced Mortar Strip under Axial Load. *Eng. Struct.* **2022**, *259*, 114191. [CrossRef]
106. Guo, L.; Deng, M.; Chen, H.; Li, R.; Ma, X.; Zhang, Y. Experimental Study on Pre-Damaged RC Beams Shear-Strengthened with Textile-Reinforced Mortar (TRM). *Eng. Struct.* **2022**, *256*, 113956. [CrossRef]
107. Dong, Z.; Deng, M.; Dai, J.; Ma, P. Diagonal Compressive Behavior of Unreinforced Masonry Walls Strengthened with Textile Reinforced Mortar Added with Short PVA Fibers. *Eng. Struct.* **2021**, *246*, 113034. [CrossRef]
108. Pinto, J.; Peixoto, A.; Vieira, J.; Fernandes, L.; Morais, J.; Cunha, V.M.C.F.; Varum, H. Render Reinforced with Textile Threads. *Constr. Build. Mater.* **2013**, *40*, 26–32. [CrossRef]
109. de Oliveira, E.M.; Machado de Oliveira, E.; de Oliveira, C.M.; Dal-Bó, A.G.; Peterson, M. Study of the Incorporation of Fabric Shavings from the Clothing Industry in Coating Mortars. *J. Clean. Prod.* **2021**, *279*, 123730. [CrossRef]
110. Truong, V.D.; Park, J.K.; Lee, S.Y.; Han, T.H.; Kim, D.J. Feasibility of Hybrid Waste Fishing Net Textile and Fiber Reinforced Cementitious Composites in Strengthening Concrete and Retrofitting Damaged Concrete. *J. Build. Eng.* **2023**, *74*, 106926. [CrossRef]
111. Dinh, N.H.; Pham, H.H.; Kim, S.H.; Choi, K.K. Tensile Performance and Cracking Characteristics of Sustainable Textile-Reinforced Cementitious Composites Utilizing Expanded Glass Aggregate and Fly Ash Replacement. *Constr. Build. Mater.* **2024**, *425*, 136084. [CrossRef]
112. Fernandes, I.V.; Lima, V.M.E.; Nascimento, C.F.G.; Carvalho, H.G.; Santos, C.L.L.; Melo Neto, A.A. Valorization of Textile Sludge for Use as Supplementary Cementitious Material—Benefiting Processes, Pozzolanic Activity, and Application in No-Slump Concrete. *Constr. Build. Mater.* **2025**, *458*, 139619. [CrossRef]
113. Pham, H.H.; Dinh, N.H.; Choi, K.K. Tensile Behavior of Lightweight Carbon Textile-Reinforced Cementitious Composites with Dispersed Fibers. *Constr. Build. Mater.* **2023**, *384*, 131455. [CrossRef]
114. Zhang, Q.; Alexis Salazar Sazon, T.; Skaug Fadnes, F.; Peng, X.; Ahmed, N.; Nikpey, H.; Mansouri, M.; Assadi, M. Design Optimization of the Cooling Systems with PCM-to-Air Heat Exchanger for the Energy Saving of the Residential Buildings. *Energy Convers. Manag. X* **2024**, *23*, 100630. [CrossRef]
115. Dallaire, J.; Adeel Hassan, H.M.; Bjernemose, J.H.; Rudolph Hansen, M.P.; Lund, I.; Veje, C.T. Performance Analysis of a Dual-Stack Air-PCM Heat Exchanger with Novel Air Flow Configuration for Cooling Applications in Buildings. *Build. Environ.* **2022**, *223*, 109450. [CrossRef]
116. Simon, F.; Ruiz-Valero, L.; Girard, A.; Galleguillos, H. Experimental and Numerical Analysis of a PCM-Integrated Roof for Higher Thermal Performance of Buildings. *J. Therm. Sci.* **2024**, *33*, 522–536. [CrossRef]
117. *EN 197-1*; Cement—Part 1: Composition, Specifications and Conformity Criteria for Common Cements Ciment. European Committee for Standardization: Brussels, Belgium, 1992.
118. *EN 1015-2*; Methods of Testing Mortars for Masonry—Part 2: Bulk Sampling of Mortars and Preparation of Mortars for Testing. European Committee for Standardization: Brussels, Belgium, 1999.
119. *EN 1015-3*; Methods of Test for Mortar for Masonry—Part 3: Determination of Consistence of Fresh Mortar (by Flow Table). European Committee for Standardization: Brussels, Belgium, 1999.
120. *EN 1015-6*; Methods of Test for Mortar for Masonry—Part 6. Determination of Bulk Density of Fresh Mortar. European Committee for Standardization: Brussels, Belgium, 1998.
121. *EN 1015-10*; Methods of Test for Mortar for Masonry—Part 10: Determination of Dry Bulk Density of Hardened Mortar. European Committee for Standardization: Brussels, Belgium, 1999.
122. *EN 1015-11*; Methods of Test for Mortar for Masonry—Part 11: Determination of Flexural and Compressive Strength of Hardened Mortar. European Committee for Standardization: Brussels, Belgium, 2020.
123. Bigg, D.M. Thermal Conductivity of Heterophase Polymer Compositions. In *Thermal and Electrical Conductivity of Polymer Material*; Springer: Berlin/Heidelberg, Germany, 1995; Volume 119.

124. Progelhof, R.C.; Throne, J.L.; Ruetsch, R.R. Methods for Predicting the Thermal Conductivity of Composite Systems: A Review. *Polym. Eng. Sci.* **1976**, *76*, 615–625. [CrossRef]
125. Kumlutas, D.; Tavman, I.H. A Numerical and Experimental Study on Thermal Conductivity of Particle Filled Polymer Composites. *J. Thermoplast. Compos. Mater.* **2006**, *19*, 441–455. [CrossRef]
126. Rayleigh, L. On the Influence of Obstacles Arranged in Rectangular Order upon the Properties of a Medium. *Lond. Edinb. Dublin Philos. Mag. J. Sci.* **1892**, *34*, 481–502. [CrossRef]
127. Hatta, H.; Taya, M. Effective Thermal Conductivity of a Misoriented Short Fiber Composite. *J. Appl. Phys.* **1985**, *58*, 2478–2486. [CrossRef]
128. Hatta, H.; Taya, M. Thermal Conductivity of Coated Filler Composites. *J. Appl. Phys.* **1986**, *59*, 1851–1860. [CrossRef]
129. Lewis, T.B.; Nielsen, L.E. Dynamic Mechanical Properties of Particulate-Filled Composites. *J. Appl. Polym. Sci.* **1970**, *14*, 1449–1471. [CrossRef]
130. Nielsen, L.E. Thermal Conductivity of Particulate-Filled Polymers. *J. Appl. Polym. Sci.* **1973**, *17*, 3819–3820. [CrossRef]
131. Bigg, D.M. Thermally Conductive Polymer Compositions. *Polym. Compos.* **1986**, *7*, 125–140. [CrossRef]
132. de Souza Kazmierczak, C.; Dutra Schneider, S.; Aguilera, O.; Albert, C.C.; Mancio, M. Rendering Mortars with Crumb Rubber: Mechanical Strength, Thermal and Fire Properties and Durability Behaviour. *Constr. Build. Mater.* **2020**, *253*, 119002. [CrossRef]
133. Akyuncu, V.; Sanliturk, F. Investigation of Physical and Mechanical Properties of Mortars Produced by Polymer Coated Perlite Aggregate. *J. Build. Eng.* **2021**, *38*, 102182. [CrossRef]
134. Ayed, R.; Bouadila, S.; Lazaar, M.; Dellagi, A.; Cabeza, L.F. Improving the Thermal and Mechanical Performance of Cement-Based Mortars for Reinforcing Masonry Structures: Computational and Experimental Methods. *Energy Effic.* **2024**, *17*, 80. [CrossRef]
135. Brooks, A.L.; Zhou, H.; Hanna, D. Comparative Study of the Mechanical and Thermal Properties of Lightweight Cementitious Composites. *Constr. Build. Mater.* **2018**, *159*, 316–328. [CrossRef]
136. Omrani, H.; Hassini, L.; Benazzouk, A.; Beji, H.; ELCafsi, A. Elaboration and Characterization of Clay-Sand Composite Based on Juncus Acutus Fibers. *Constr. Build. Mater.* **2020**, *238*, 117712. [CrossRef]
137. Kanagalakhmi, A.S.; Indhuja, B.; Rithisri, U.; Devi, R.P.K. Study on Human Hair in Concrete as a Fiber Reinforcement. *J. Emerg. Technol. Innov. Res.* **2021**, *8*, 173–181.
138. Alyousef, R. Enhanced Acoustic Properties of Concrete Composites Comprising Modified Waste Sheep Wool Fibers. *J. Build. Eng.* **2022**, *56*, 104815. [CrossRef]
139. Charai, M.; Mghazli, M.O.; Channouf, S.; El hammouti, A.; Jagadesh, P.; Moga, L.; Mezrhab, A. Lightweight Waste-Based Gypsum Composites for Building Temperature and Moisture Control Using Coal Fly Ash and Plant Fibers. *Constr. Build. Mater.* **2023**, *393*, 132092. [CrossRef]
140. Rashad, A.M.; Mosleh, Y.A.; Mokhtar, M.M. Thermal Insulation and Durability of Alkali-Activated Lightweight Slag Mortar Modified with Silica Fume and Fly Ash. *Constr. Build. Mater.* **2024**, *411*, 134255. [CrossRef]
141. *ISO 14001*; Environmental Management System, Requirements with Guidelines for Use. International Organization for Standardization (ISO): Geneva, Switzerland, 2005.
142. *ASHRAE 90.1*; Energy Standard for Buildings Except Low-Rise Residential Buildings. American Society of Heating, Refrigerating, and Air-Conditioning Engineers (ASHRAE): Atlanta, GA, USA, 2022.
143. *ISO 13790:2008*; Energy Performance of Buildings—Calculation of Energy Use for Space Heating and Cooling. International Organization for Standardization (ISO): Geneva, Switzerland, 2008.

Disclaimer/Publisher's Note: The statements, opinions and data contained in all publications are solely those of the individual author(s) and contributor(s) and not of MDPI and/or the editor(s). MDPI and/or the editor(s) disclaim responsibility for any injury to people or property resulting from any ideas, methods, instructions or products referred to in the content.